Chapter V
Extension to Linear Elastic Fracture Mechanics

Content

Summary

In this chapter, the natural neighbours method is extended to the domain of 2D Linear Elastic Fracture Mechanics (LEFM) using an approach based on the FRAEIJS de VEUBEKE variational principle which allows independent assumptions on the displacement field, the stresses filed, the strain field and the surface distributed support reactions field.

The 2D domain contains *N* nodes (including nodes on the domain contour and nodes located at each crack tip) and the *N* Voronoi cells corresponding these nodes are built.

The cells corresponding to the crack tip nodes are called Linear Fracture Mechanics Voronoi Cells (LFMVC). The other ones are called Ordinary Cells (OVC).

A node is located at the crack tip and, in the LFMVC containing this node, the stress and the strain discretizations include not only a constant term but also additional terms corresponding to the solutions of LEFM for modes 1 and 2 [WESTERGAARD, H.M. (1939)].

The following discretization hypotheses are admitted:

1. The assumed displacements are interpolated between the nodes with the Laplace interpolation function.
2. The assumed support reactions are constant over each edge *K* of Voronoi cells on which displacements are imposed
3. The assumed stresses are constant over each OVC
4. The assumed strains are constant over each OVC
5. The assumed stresses are assumed to have the distribution corresponding to modes 1 and 2 in each LFMVC
6. The assumed strains are assumed to have the distribution corresponding to modes 1 and 2 in each LFMVC

Introducing these hypotheses in the FdV variational principle produces the set of equations governing the discretized solid.

In this approach, the stress intensity coefficients are obtained as primary variables of the solution.

These equations are recast in matrix form and it is shown that the discretization parameters associated with the assumptions on the stresses and on the strains can be eliminated at the Voronoi cell level so that the final system of equations only involves the nodal displacements, the assumed support reactions and the stress intensity coefficients.

These support reactions can be further eliminated from the equation system if the imposed support conditions only involve displacements imposed as constant (in particular displacements imposed to zero) on a part of the solid contour.

The present approach has also the following properties.

In the OVCs

1. In the absence of body forces, the calculation of integrals over the area of the domain is avoided: only integrations on the edges of the Voronoi cells are required.
2. The derivatives of the Laplace interpolation functions are not required.

In the LFMVCs,

1. Some integrations on the area of the LFMVCs are required but they can be calculated analytically.
2. The other integrals are integrals on the edges of the LFMVCs
3. The derivatives of the Laplace interpolation functions are not required

Several applications are used to evaluate the method.

Patch test, translation test, mode 1 tests, mode 2 tests and single edge crack test confirm the validity of this approach.

V.1. Introduction

In chapter III, starting from the Fraeijs de Veubeke (FdV) variational principle, a new approach of the natural neighbours method has been developed for problems of linear elasticity.

It has been extended, in chapter IV, to materially non linear problems.

In the absence of body forces ($F_i = 0$), it has been shown that for both cases:

- the calculation of integrals of the type $\int_A \bullet dA$ can be avoided; only numerical integrations on the edges of the Voronoi cells are performed;
- the derivatives of the Laplace interpolation functions are unnecessary;
- boundary conditions of the type $u_i = \tilde{u}_i$ on S_u can be imposed in the average sense in general and exactly if $\tilde{u}_i$ is linear between two contour nodes, which is obviously the case for $\tilde{u}_i = 0$;
- incompressibility locking is avoided.

The motivation of the present study is to explore if this approach can be extended to solve problems of Linear Elastic Fracture Mechanics (LEFM).

Indeed, in Linear Elastic Fracture Mechanics, the stress intensity factors play a central role and, since the FdV variational principle allows discretizing the stresses and the strains independently of the assumptions on the displacement field, it seems logical and elegant to take advantage of this flexibility and to introduce, near the crack tips, stress and strain assumptions inspired from the analytical solution provided by the Theory of Elasticity [WESTERGAARD, H.M. (1939)].

However, the properties that the numerical calculation of integrals of the type $\int_A \bullet dA$ could be avoided, that the derivatives of the Laplace interpolation functions were unnecessary and that incompressibility locking was also avoided resulted from the assumption of a constant stress field and a constant strain field in each of the Voronoi cells.

It is not obvious that these properties still hold with the non constant assumptions on the stresses and the strains near the crack tips.

These points are carefully examined in the present chapter.

On the other hand, thanks to the stress and strain assumptions used near the crack tips, the stress intensity factors corresponding to fracture modes 1 and 2 become primary variables of the numerical solution which is normally an advantage. However, it must be verified that good precision and convergence are obtained.

This is also considered in the present chapter.

It is worth recalling that the basic notions of LEFM used in the present chapter were briefly introduced in chapter II, section II.4.

V.2. State of the art

There are many numerical approaches currently available to solve problems of LEFM and, in particular, to calculate the stress intensity factors.

Research in this domain has produced a very large number of papers and it would be extremely difficult, and perhaps useless in the frame of this thesis, to extensively review the literature on this subject.

Therefore, the following state of the art only briefly mentions some of the basic references and proposes a classification of the methods in 4 categories.

V.2.1. Finite element method

Usually, displacement-type finite elements (based on the virtual work principle) are used.

Two main categories of approaches are used [INGRAFFEA A.R. and WAWRZYNEK P. (2003)]

In the "direct approach", the stress intensity factors are deduced from the displacement field. This is the case of the Crack Opening Displacement method [CHAN S.K. et al. (1970)].

In some cases, the formulation of finite elements at the crack tip can be adapted to improve the displacement field [BARSOUM R.S. (1977)].

In the "energy approach" which is generally more precise, the stress intensity factors are deduced from the energy distribution in the vicinity of the crack tip, either from the energy release as in the method of the Virtual Crack Extension [HELLEN T.K. and BLACKBURN W.S. (1975)] or from the J-integral as in the Equivalent Domain Integral Method [MORAN B. and SHIH C.F. (1987-a) & (1987-b)].

V.2.2. Boundary elements method

In this method, only the boundaries of the solid are discretized. The partial differential equations of the Theory of Elasticity are transformed into integral equations on the boundaries of the domain. Basically, the primary unknowns of the numerical problem remain the displacements.

This is the case for the "crack Green's function method" [SNYDER M.D. and CRUSE T.A. (1975)], the "displacement discontinuity method" [CROUCH S.L. (1976)] and the "subregions method" [BLANFORD G.E. et al. (1991)]

But a dual method using also the surface tractions as primary unknowns has also been developed [PORTELA A. et al.(1991)].

V.2.3. Meshless method

This method has been applied to fracture mechanics since 1994 [BELYTCHKO T. et al. (1994-b)] and, subsequently, different improvements have been introduced, for example to couple it with the finite element method [BELYTCHKO T. et al. (1996-b)], to ensure the continuity of displacements in the vicinity of the crack [ORGAN D. et al.(1996)], to improve the representation of the singularity at the crack tip [FLEMING M. et al. (1997)], to use an arbitrary Lagrangian-Eulerian formulation [PONTHOT J.P. and BELYTCHKO T. (1998)], to enrich the displacement approximation near the crack tip [LEE S.H. and YOON Y.C. (2003)] or to enrich the weighting functions [DUFLOT M. and NGUYEN D.H. (2004-a) and (2004-b)].

These approaches share the usual advantages and drawbacks of the meshless methods already mentioned in chapter II, section II.2.

V.2.4. Extended finite element methods

The extended finite element method (XFEM) [MOES N. et al. (1999)] allows discontinuities in the assumed displacement field. The discontinuities can be due to the presence of cracks and do not have to coincide with the finite element edges: they can be located anywhere in the domain independently of the finite element mesh.

Since chapter VI of this thesis will deal with a an extended natural neighbours method (XNEM) which is somehow inspired from the XFEM, we will not go further in the presentation of the XFEM here and come back on this subject in chapter VI.

V.3. Domain decomposition

In the natural neighbours method, the domain contains N nodes and the N Voronoi cells corresponding to these nodes are built.

At each crack tip, a node is located (figure V.1).

The cells corresponding to the crack tip nodes are called Linear Fracture Mechanics Voronoi Cells (LFMVC). The other ones are called Ordinary Voronoi Cells (OVC).

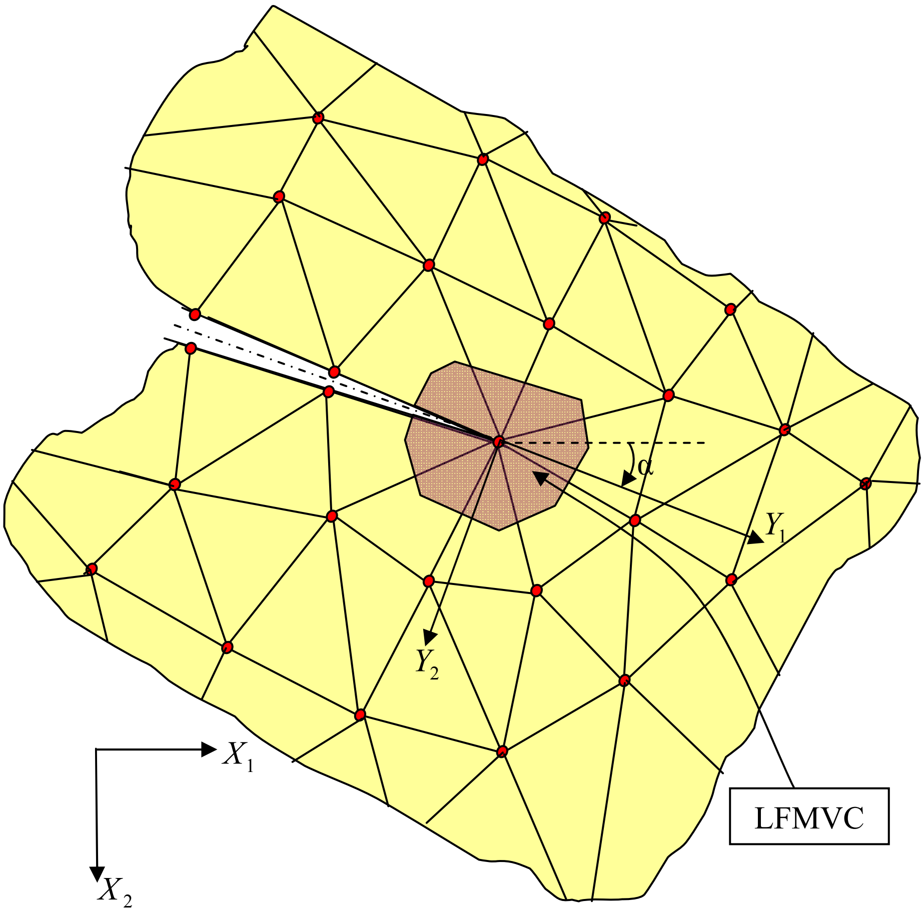

Figure V.1. A Linear Elastic Fracture Mechanics Voronoi cell (LFMVC) at a crack tip.

The area of the domain is:

$$A = \sum_{I=1}^{N} A_I \qquad \text{(V.1)}$$

with A_I the area of Voronoi cell I.

We denote C_I the contour of Voronoi cell I.

We start from the FdV variational principle introduced in chapter II and we recall its expression for completeness (we keep the equation numbers of chapter II).

$$\delta\Pi = \int_A (\sigma_{ij} - \Sigma_{ij})\delta\varepsilon_{ij} dA - \int_A (\frac{\partial \Sigma_{ji}}{\partial X_j} + F_i)\delta u_i\, dA + \int_A \delta\Sigma_{ij}\left[\frac{1}{2}(\frac{\partial u_i}{\partial X_j} + \frac{\partial u_j}{\partial X_i}) - \varepsilon_{ij}\right] dA$$

$$+ \int_{S_u} (N_j \Sigma_{ji} - r_i)\delta u_i\, dS + \int_{S_t} (N_j \Sigma_{ji} - T_i)\delta u_i\, dS = 0 \qquad \text{(II.36)}$$

or

$$\delta\Pi = \delta\Pi_1 + \delta\Pi_2 + \delta\Pi_3 + \delta\Pi_4 + \delta\Pi_5 + \delta\Pi_6 = 0 \qquad \text{(II.31)}$$

with the different terms

$$\delta\Pi_1 = \int_A \delta W(\varepsilon_{ij}) dA = \int_A \sigma_{ij}\delta\varepsilon_{ij} dA \qquad \text{(II.25)}$$

$$\delta\Pi_2 = \int_A \Sigma_{ij}\left[\frac{1}{2}(\frac{\partial \delta u_i}{\partial X_j} + \frac{\partial \delta u_j}{\partial X_i}) - \delta\varepsilon_{ij}\right] dA \qquad \text{(II.26)}$$

$$\delta\Pi_3 = \int_A \delta\Sigma_{ij}\left[\frac{1}{2}(\frac{\partial u_i}{\partial X_j} + \frac{\partial u_j}{\partial X_i}) - \varepsilon_{ij}\right] dA \qquad \text{(II.27)}$$

$$\delta\Pi_4 = -\int_A F_i\, \delta u_i\, dA \qquad \text{(II.28)}$$

$$\delta\Pi_5 = -\int_{S_t} T_i\, \delta u_i\, dS \qquad \text{(II.29)}$$

$$\delta\Pi_6 = \int_{S_u} \delta r_i(\tilde{u}_i - u_i) dS - \int_{S_u} r_i\, \delta u_i\, dS \qquad \text{(II.30)}$$

For the linear elastic case, the stresses are given by:

$$\sigma_{ij} = \frac{\partial W(\varepsilon_{ij})}{\partial \varepsilon_{ij}} \qquad \text{(II.34)}$$

and

$$W(\varepsilon_{ij}) = \frac{1}{2} C_{ijkl}\, \varepsilon_{ij}\, \varepsilon_{kl} \qquad \text{(II.35)}$$

where C_{ijkl} is the classical Hooke's tensor.

In (II.29) and (II.30), the integrals are computed along the domain contour. This contour is the union of some of the edges of the exterior Voronoi cells. These edges are denoted by S_K and we have

$$S=\sum_{K=1}^{M} S_K\ ; \quad S_u=\sum_{K=1}^{M_u} S_K\ ; \quad S_t=\sum_{K=1}^{M_t} S_K\ ; \qquad S=S_u \cup S_t \Rightarrow M=M_u+M_t \qquad \text{(V.2)}$$

where M is the number of edges composing the contour, M_u the number of edges on which displacements $\widetilde{u}_i$ are imposed and M_t the number of edges on which surface tractions T_i are imposed.

Using the above domain decomposition, these terms become:

$$\delta\Pi_1=\sum_{I=1}^{N}\int_{A_I}\sigma_{ij}\delta\varepsilon_{ij}\,dA_I \qquad \text{(V. 3)}$$

$$\delta\Pi_2=\sum_{I=1}^{N}\int_{A_I}\Sigma_{ij}\left[\frac{1}{2}\left(\frac{\partial\delta u_i}{\partial X_j}+\frac{\partial\delta u_j}{\partial X_i}\right)-\delta\varepsilon_{ij}\right]dA_I \qquad \text{(V. 4)}$$

$$\delta\Pi_3=\sum_{I=1}^{N}\int_{A_I}\delta\Sigma_{ij}\left[\frac{1}{2}\left(\frac{\partial u_i}{\partial X_j}+\frac{\partial u_j}{\partial X_i}\right)-\varepsilon_{ij}\right]dA_I \qquad \text{(V. 5)}$$

$$\delta\Pi_4=-\sum_{I=1}^{N}\int_{A_I}F_i\,\delta u_i\,dA_I \qquad \text{(V. 6)}$$

$$\delta\Pi_5=-\sum_{K=1}^{M_t}\int_{S_K}T_i\,\delta u_i\,dS_K \qquad \text{(V. 7)}$$

$$\delta\Pi_6=\sum_{K=1}^{M_u}\left[\int_{S_K}\delta r_i(\widetilde{u}_i-u_i)\,dS_K-\int_{S_K}r_i\,\delta u_i\,dS_K\right] \qquad \text{(V. 8)}$$

V.4. Discretization

We make the following discretization hypotheses in the OVCs:

1. The assumed strains ε_{ij} are constant over each Voronoi cell I:

$$\varepsilon_{ij}=\varepsilon_{ij}^{I} \qquad \text{(V. 9)}$$

2. The asumed stresses Σ_{ij} are constant over each Voronoi cell I:

$$\Sigma_{ij}=\Sigma_{ij}^{I} \qquad \text{(V.10)}$$

3. The assumed support reactions r_i are constant over each edge K of Voronoi cells on which displacements are imposed:

$$r_i=r_i^{K} \qquad \text{(V. 11)}$$

4. The assumed displacements u_i are interpolated by Laplace interpolation functions:

$$u_i=\sum_{J=1}^{N}\Phi_J u_i^{J} \qquad \text{(V. 12)}$$

where u_i^J is the displacement of node J (corresponding to the Voronoi cell J).

For the LFMVCs we use the results of Linear Elastic Fracture Mechanics.

The stress fields near the crack tip (figure V.2, $r <<<$) are given in the local reference system (Y_1, Y_2) by Westergaard [WESTERGAARD, H.M. (1939)].

for mode 1:
$$\begin{Bmatrix} \tau_{11} \\ \tau_{22} \\ \tau_{12} \end{Bmatrix} = \frac{K_1}{\sqrt{2\pi r}} cos\frac{\theta}{2} \begin{Bmatrix} 1 - sin\frac{\theta}{2} \quad sin\frac{3\theta}{2} \\ 1 + sin\frac{\theta}{2} \quad sin\frac{3\theta}{2} \\ sin\frac{\theta}{2} \quad cos\frac{3\theta}{2} \end{Bmatrix} \qquad (V.13)$$

for mode 2:
$$\begin{Bmatrix} \tau_{11} \\ \tau_{22} \\ \tau_{12} \end{Bmatrix} = \frac{K_2}{\sqrt{2\pi r}} \begin{Bmatrix} -sin\frac{\theta}{2}(2 + cos\frac{\theta}{2} \quad cos\frac{3\theta}{2}) \\ cos\frac{\theta}{2} sin\frac{\theta}{2} \quad cos\frac{3\theta}{2} \\ cos\frac{\theta}{2}(1 - sin\frac{\theta}{2} \quad sin\frac{3\theta}{2}) \end{Bmatrix} \qquad (V.14)$$

K_1 and K_2 are the stress intensity factors of modes 1 and 2 respectively.

In the simple loading cases of figure V.2, they are given by:

$$K_1 = \sigma_\infty \sqrt{\pi a} \qquad (V.15)$$

$$K_2 = \tau_\infty \sqrt{\pi a} \qquad (V.16)$$

These stresses are valid for both plane stress and plane strain conditions.

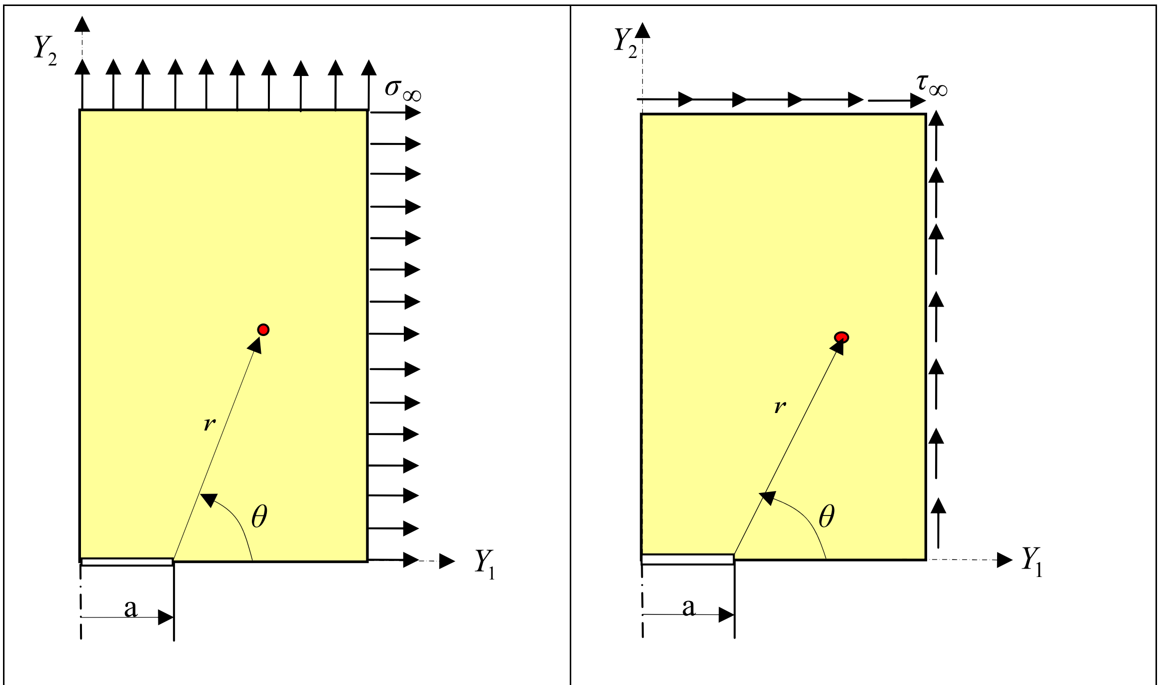

a. Mode 1: simple tension | b. Mode 2: pure shear

Figure V.2. Modes 1 and 2 of fracture mechanics.
Crack tip coordinates (one quarter of the plate represented)

The LFMVCs are discretized as follows:

The assumed displacements v_i are interpolated in the local reference system (Y_1,Y_2) by the Laplace interpolant as in the OVCs:

$$v_i = \sum_{J=1}^{N} \Phi_J v_i^J \tag{V.17}$$

where v_1, v_2 are the components of the displacement at a point in the LFMVC with respect to (Y_1,Y_2).

The assumed stresses are interpolated in the local reference system (Y_1,Y_2) shown on figure V.1. by:

$$\begin{Bmatrix} P_{11} \\ P_{22} \\ P_{12} \end{Bmatrix} = \begin{Bmatrix} P_{11}^O \\ P_{22}^O \\ P_{12}^O \end{Bmatrix} + f(r)\left[K_{\Sigma 1}\{g_1(\theta)\} + K_{\Sigma 2}\{g_2(\theta)\}\right] \quad \Leftrightarrow \quad \{P\} = \{P^O\} + \{P^F\} \tag{V.18}$$

with

$$\{P^F\} = K_{\Sigma 1}\{H^{\Sigma 1}\} + K_{\Sigma 2}\{H^{\Sigma 2}\} \tag{V.19}$$

$$\{H^{\Sigma 1}\} = \begin{Bmatrix} H_{11}^{\Sigma 1} \\ H_{22}^{\Sigma 1} \\ H_{12}^{\Sigma 1} \end{Bmatrix} = f(r)\{g_1(\theta)\} \tag{V.20}$$

$$\{H^{\Sigma 2}\} = \begin{Bmatrix} H_{11}^{\Sigma 2} \\ H_{22}^{\Sigma 2} \\ H_{12}^{\Sigma 2} \end{Bmatrix} = f(r)\{g_2(\theta)\} \tag{V.21}$$

$$\{g_1(\theta)\} = cos\frac{\theta}{2} \begin{Bmatrix} 1 - sin\frac{\theta}{2}\ sin\frac{3\theta}{2} \\ 1 + sin\frac{\theta}{2}\ sin\frac{3\theta}{2} \\ sin\frac{\theta}{2}\ cos\frac{3\theta}{2} \end{Bmatrix} \tag{V.22}$$

$$\{g_2(\theta)\} = \begin{Bmatrix} -sin\frac{\theta}{2}(2 + cos\frac{\theta}{2}\ cos\frac{3\theta}{2}) \\ cos\frac{\theta}{2} sin\frac{\theta}{2}\ cos\frac{3\theta}{2} \\ cos\frac{\theta}{2}(1 - sin\frac{\theta}{2}\ sin\frac{3\theta}{2}) \end{Bmatrix} \tag{V.23}$$

$$f(r) = \frac{1}{\sqrt{2\pi r}} \tag{V.24}$$

$K_{\Sigma 1}$ and $K_{\Sigma 2}$ can be considered as generalized stresses (or stress parameters) associated with the considered LFMVC.

The assumed strains are interpolated in the local reference system (Y_1, Y_2) by:

$$\begin{Bmatrix} \gamma_{11} \\ \gamma_{22} \\ 2\gamma_{12} \end{Bmatrix} = \begin{Bmatrix} \gamma_{11}^O \\ \gamma_{22}^O \\ 2\gamma_{12}^O \end{Bmatrix} + \frac{1}{E^*} \begin{bmatrix} 1 & -\nu^* & 0 \\ -\nu^* & 1 & 0 \\ 0 & 0 & 2(1+\nu^*) \end{bmatrix} \begin{Bmatrix} P_{11}^F \\ P_{22}^F \\ P_{12}^F \end{Bmatrix} \Leftrightarrow \{\gamma\} = \{\gamma^O\} + [D]\{P^F\} \qquad \text{(V.25)}$$

with
$$E^* = \begin{cases} \dfrac{E}{1-\nu^2} & \text{in plane strain state} \\ E & \text{in plane stress state} \end{cases} \qquad \nu^* = \begin{cases} \dfrac{\nu}{1-\nu} & \text{in plane strain state} \\ \nu & \text{in plane stress state} \end{cases}$$

The assumed support tractions r_i are constant over each edge K of Voronoi cells on which displacements are imposed:

$$r_i = r_i^K \qquad \text{(V.26)}$$

Usually, the lips of the fracture are not submitted to imposed displacements. In such a case, (V.26) is useless in a LFMVC.

The assumption (V.25) implies a priori that, in the LFMVC, $\sigma_{ij} = \Sigma_{ij}$.

In a given problem, there could be N_C crack tips.

For the sake of simplicity, the LFMVCs will be numbered from 1 to N_C and the OVCs are numbered from $N_C + 1$ to N.

The introduction of these assumptions in the FdV variational principle (II.31) leads to the equations of table V.2 with the notations of table V.1.

The details of the calculations are given in annex 2.

Table V.1. Matrix notations for the Linear Elastic Fracture Mechanics case	
Notations and symbols	**Comments**
$[R]^I = \begin{bmatrix} \cos\alpha^I & \sin\alpha^I \\ -\sin\alpha^I & \cos\alpha^I \end{bmatrix}$; $\begin{Bmatrix} v_1 \\ v_2 \end{Bmatrix} = [R]^I \begin{Bmatrix} u_1 \\ u_2 \end{Bmatrix}$	Rotation matrix between (X_1, X_2) and $(Y_1, Y_2)^I$ (figure 1)
$\{\varepsilon\}^I = \begin{Bmatrix} \varepsilon_{11}^I \\ \varepsilon_{22}^I \\ 2\varepsilon_{12}^I \end{Bmatrix}$ $\quad \langle\varepsilon\rangle^I = \langle \varepsilon_{11}^I \;\; \varepsilon_{22}^I \;\; 2\varepsilon_{12}^I \rangle$	Strains in OVC ($I = N_C + 1, N$)

$\{\gamma\}^I = \begin{Bmatrix} \gamma_{11}^I \\ \gamma_{22}^I \\ 2\gamma_{12}^I \end{Bmatrix} \quad \langle\gamma\rangle^I = \langle \gamma_{11}^I \quad \gamma_{22}^I \quad 2\gamma_{12}^I \rangle$	Strains in LFMVC ($I = 1, N_C$) with respect to its local reference system $(Y_1, Y_2)^I$
$\{\sigma\}^I = \begin{Bmatrix} \sigma_{11}^I \\ \sigma_{22}^I \\ \sigma_{12}^I \end{Bmatrix} \quad \langle\sigma\rangle^I = \langle \sigma_{11}^I \quad \sigma_{22}^I \quad 2\sigma_{12}^I \rangle$	Stresses in OVC ($I = N_C + 1, N$)
$\{P\}^I = \begin{Bmatrix} P_{11}^I \\ P_{22}^I \\ P_{12}^I \end{Bmatrix} \quad \langle P\rangle^I = \langle P_{11}^I \quad P_{22}^I \quad 2P_{12}^I \rangle$	Stresses in LFMVC , ($I = 1, N_C$) with respect to its local reference system $(Y_1, Y_2)^I$
$\{K_\Sigma\}^I = \begin{Bmatrix} K_{\Sigma 1}^I \\ K_{\Sigma 2}^I \end{Bmatrix} \quad \langle K_\Sigma\rangle^I = \langle K_{\Sigma 1}^I \quad K_{\Sigma 2}^I \rangle$	Generalized stresses or stress parameters in the LFMVC ($I = 1, N_C$)
$\{u\}^I = \begin{Bmatrix} u_1^I \\ u_2^I \end{Bmatrix} \quad \langle u\rangle^I = \langle u_1^I \quad u_2^I \rangle$	Displacements of node I belonging to cell I ($I = N_C + 1, N$)
$\{v\}^I = \begin{Bmatrix} v_1^I \\ v_2^I \end{Bmatrix} \quad \langle v\rangle^I = \langle v_1^I \quad v_2^I \rangle$	Displacements of node I belonging to cell I ($I = 1, N_C$) with respect to the local reference system $(Y_1, Y_2)^I$
$A_I \;;\; C_I$	Area and contour of cell I
$K(I)$	Edge K of cell I
Φ_J	Laplace function (J=1,N)
$\tilde{F}_i^{IJ} = \int_{A_I} F_i \Phi_J \, dA_I \;;\; \{\tilde{F}\}^{IJ} = \begin{Bmatrix} \tilde{F}_1^{IJ} \\ \tilde{F}_2^{IJ} \end{Bmatrix} \quad \{\tilde{F}\}^J = \sum_{I=1}^{N} \{\tilde{F}\}^{IJ}$	$\{\tilde{F}\}^J$ is the nodal force at node J equivalent to the body forces F_i
$\tilde{T}_i^{KJ} = \int_{S_K} T_i \Phi_J \, dS_K \;;\; \{\tilde{T}\}^{KJ} = \begin{Bmatrix} \tilde{T}_1^{KJ} \\ \tilde{T}_2^{KJ} \end{Bmatrix} ; \{\tilde{T}\}^J = \sum_{K=1}^{M_t} \{\tilde{T}\}^{KJ}$	$\{\tilde{T}\}^J$ is the nodal force at node J equivalent to the surface tractions T_i
$\{r\}^J = \sum_{K=1}^{M_u} r_i^K B^{KJ}$	$\{r\}^J$ is the nodal force at node J equivalent to the assumed surface support reactions on S_u
$\tilde{U}_i^K = \int_{S_K} \tilde{u}_i dS_K \;;\; \{\tilde{U}\}^K = \begin{Bmatrix} \tilde{U}_2^K \\ \tilde{U}_1^K \end{Bmatrix}$	$\{\tilde{U}\}^K$ is a generalized displacement taking account of imposed displacements $\tilde{u}_i$ on edge K
$B^{KJ} = \int_{S_K} \Phi_J \, dS_K$	Integration over the edge K of a cell

$A_j^{IJ} = \oint_{C_I} N_j^I \Phi_J \, dC_I$; $[A]^{IJ} = \begin{bmatrix} A_1^{IJ} & 0 & A_2^{IJ} \\ 0 & A_2^{IJ} & A_1^{IJ} \end{bmatrix}$	A_j^{IJ} can also be computed by $A_j^{IJ} = \sum_{all\,K(I)} N_j^{K(I)} B^{K(I)J}$
$[\partial\Phi]^J = \begin{bmatrix} \frac{\partial\Phi_J}{\partial Y_1} & 0 \\ 0 & \frac{\partial\Phi_J}{\partial Y_2} \\ \frac{\partial\Phi_J}{\partial Y_2} & \frac{\partial\Phi_J}{\partial Y_1} \end{bmatrix}$	Derivatives of Laplace function (J=1,N)
$\{H^{\Sigma 1}\} = f(r)\{g_1(\theta)\}$; $\{H^{\Sigma 2}\} = f(r)\{g_2(\theta)\}$	Stress functions in a LFMVC
$\{w_1\}^{IJ} = \int_{A_I} [\partial\Phi]^{J,T} \{H^{\Sigma 1}\} dA_I$; $\{w_2\}^{IJ} = \int_{A_I} [\partial\Phi]^{J,T} \{H^{\Sigma 2}\} dA_I$; $[W]^{IJ} = \lfloor \{w_1\}^{IJ} \quad \{w_2\}^{IJ} \rfloor$	$[W]^{IJ}$ is an influence matrix such that $[W]^{IJ}\{u\}^J$ gives the contribution of the displacements at node J on the generalized strains in the LFMVCs
$\{\sigma\}^I = [C]^I\{\varepsilon\}^I \Leftrightarrow \{\varepsilon\}^I = [D]^I\{\sigma\}^I$, $I = 1, N$	Hooke's law for cell I
$[V]^I = \begin{bmatrix} \int_{A_I} \langle H^{\Sigma 1}\rangle [D]^I \{H^{\Sigma 1}\} dA_I & \int_{A_I} \langle H^{\Sigma 1}\rangle [D]^I \{H^{\Sigma 2}\} dA_I \\ \int_{A_I} \langle H^{\Sigma 2}\rangle [D]^I \{H^{\Sigma 1}\} dA_I & \int_{A_I} \langle H^{\Sigma 2}\rangle [D]^I \{H^{\Sigma 2}\} dA_I \end{bmatrix}$	
$\{e^\gamma\}^I = \begin{Bmatrix} e_1^\gamma \\ e_2^\gamma \end{Bmatrix}^I = \begin{Bmatrix} \int_{A_I} \langle H^{\Sigma 1}\rangle \{\gamma^0\} dA_I \\ \int_{A_I} \langle H^{\Sigma 2}\rangle \{\gamma^0\} dA_I \end{Bmatrix} = [IH]^I \{\gamma^0\}^I$	$[IH]^I = \begin{Bmatrix} \int_{A_I} \langle H^{\Sigma 1}\rangle dA_I \\ \int_{A_I} \langle H^{\Sigma 2}\rangle dA_I \end{Bmatrix}$ $I = 1, N_C$
$\{e^0\}^I = \begin{Bmatrix} e_1^0 \\ e_2^0 \end{Bmatrix}^I = \begin{Bmatrix} \int_{A_I} \langle P^0\rangle^I [D]^I \{H^{\Sigma 1}\} dA_I \\ \int_{A_I} \langle P^0\rangle^I [D]^I \{H^{\Sigma 2}\} dA_I \end{Bmatrix} = [IH]^I [D]^I \{P^0\}^I$	
$\{e\}^I = \begin{Bmatrix} e_1 \\ e_2 \end{Bmatrix}^I = \begin{Bmatrix} \int_{A_I} \langle\tau\rangle^I [D]^I \{H^{\Sigma 1}\} dA_I \\ \int_{A_I} \langle\tau\rangle^I [D]^I \{H^{\Sigma 2}\} dA_I \end{Bmatrix} = [IH]^I [D]^I \{\tau\}^I$	

Table V.2. Discretized equations in matrix form for the linear elastic fracture mechanics case.		
Equations	Comments	
$\{e\}^I = \{e^0\}^I + \{e^\gamma\}^I + 2[V]^I\{K_\Sigma\} - \sum_{J=1}^{N}[W]^{IJ,T}[R]^I\{u\}^J$, $I = 1, N_C$	Compatibility equations for the LFMVCs	(V.27)
$\{\sigma\}^I = \{\Sigma\}^I, \quad I = N_C + 1, N$	Constitutive stresses in OVCs	(V.28)
$\{\tau\}^I = \{P\}^I, \quad I = 1, N_C$	Constitutive stresses in LFMVCs	(V.29)
$A_I\{\varepsilon\}^I = \sum_{J=1}^{N}[A]^{IJ,T}\{u\}^J, \quad I = N_C + 1, N$	Compatibility equation for the OVCs	(V.30)
$\sum_{I=1}^{N_C}\left\{[R]^{I,T}[W]^{IJ}\{K_\Sigma\}^I + \int_{A_I}[R]^{I,T}[\partial\Phi]^{J,T}\{P^0\}^I dA_I\right\}$ $+\sum_{I=N_C+1}^{N}[A]^{IJ}\{\Sigma\}^I - \{\tilde{F}\}^J - \{\tilde{T}\}^J - \sum_{K=1}^{M_u}B^{KJ}\{r\}^K = 0, \quad J = 1, N$	Equilibrium equation for each Voronoi cell	(V.31)
$A_I\{\gamma^0\}^I + \int_{A_I}\left[K_{\Sigma 1}^I[D]^I\{H^{\Sigma 1}\} + K_{\Sigma 2}^I[D]^I\{H^{\Sigma 2}\}\right]dA_I$ $= \sum_{J=1}^{N}\int_{A_I}[\partial\Phi]^J dA_I\,[R]^I\{u\}^J, \quad I = 1, N_C$	Average strain of LFM for the LFMVCs	(V.32)
$\sum_{J=1}^{N}B^{KJ}\{u\}^J = \{\tilde{U}\}^K, \quad K = 1, M_u$	Compatibility equation on edge K	(V.33)

It is seen that, in the absence of body forces, the only terms that require an integration over the area of a LFMVC are $\{w_1\}^{IJ}$, $\{w_2\}^{IJ}$, $[V]^I$, $[IH]$ and $\sum_{J=1}^{N}\int_{A_I}[\partial\Phi]^J dA_I\,[R]^I\{u\}^J$ in (V.32).

In order to avoid the calculation of the derivatives of the Laplace interpolation function in $\{w_1\}^{IJ}$ and $\{w_2\}^{IJ}$, an integration by part is performed.

$$\{w_1\}^{IJ} = \int_{A_I}[\partial\Phi]^{J,T}\{H^{\Sigma 1}\}dA_I = \oint_{C_I}\Phi_J[M]^{I,T}\{H^{\Sigma 1}\}dC_I - \int_{A_I}\Phi_J\{\partial H^{\Sigma 1}\}dA \qquad \text{(V.34)}$$

$$\{w_2\}^{IJ} = \int_{A_I} [\partial\Phi]^{J,T} \left\{H^{\Sigma 2}\right\} dA_I = \oint_{C_I} \Phi_J [M]^{I,T} \left\{H^{\Sigma 2}\right\} dC_I - \int_{A_I} \Phi_J \left\{\partial H^{\Sigma 2}\right\} dA_I \quad \text{(V.35)}$$

with

$$[M]^I = \begin{bmatrix} M_1^I & 0 \\ 0 & M_2^I \\ M_2^I & M_1^I \end{bmatrix} \; ; \; \left\{\partial H^{\Sigma 1}\right\} = \begin{Bmatrix} \dfrac{\partial H_{11}^{\Sigma 1}}{\partial Y_1} + \dfrac{\partial H_{12}^{\Sigma 1}}{\partial Y_2} \\ \\ \dfrac{\partial H_{12}^{\Sigma 1}}{\partial Y_1} + \dfrac{\partial H_{22}^{\Sigma 1}}{\partial Y_2} \end{Bmatrix} \; ; \; \left\{\partial H^{\Sigma 2}\right\} = \begin{Bmatrix} \dfrac{\partial H_{11}^{\Sigma 2}}{\partial Y_1} + \dfrac{\partial H_{12}^{\Sigma 2}}{\partial Y_2} \\ \\ \dfrac{\partial H_{12}^{\Sigma 2}}{\partial Y_1} + \dfrac{\partial H_{22}^{\Sigma 2}}{\partial Y_2} \end{Bmatrix} \quad \text{(V.36)}$$

where M_1^I and M_2^I are the 2 components of the outside normal to the contour of the LFMVC with respect to the local reference system (Y_1, Y_2),.

However, since the stresses (V.13, V.14) introduced in the assumption (V.18) constitute a solution of the Theory of Elasticity, they satisfy the equilibrium equations:

$$\frac{\partial \tau_{11}}{\partial Y_1} + \frac{\partial \tau_{12}}{\partial Y_2} = 0 \quad \Rightarrow \quad \frac{\partial H_{11}^{\Sigma 1}}{\partial Y_1} + \frac{\partial H_{12}^{\Sigma 1}}{\partial Y_2} = 0 \quad \text{(V.37)}$$

$$\frac{\partial \tau_{12}}{\partial Y_1} + \frac{\partial \tau_{22}}{\partial Y_2} = 0 \quad \Rightarrow \quad \frac{\partial H_{12}^{\Sigma 1}}{\partial Y_1} + \frac{\partial H_{22}^{\Sigma 1}}{\partial Y_2} = 0 \quad \text{(V.38)}$$

Consequently

$$\{w_1\}^{IJ} = \int_{A_I} [\partial\Phi]^{J,T} \left\{H^{\Sigma 1}\right\} dA_I = \oint_{C_I} \Phi_J [M]^{I,T} \left\{H^{\Sigma 1}\right\} dC_I \quad \text{(V.39)}$$

$$\{w_2\}^{IJ} = \int_{A_I} [\partial\Phi]^{J,T} \left\{H^{\Sigma 2}\right\} dA_I = \oint_{C_I} \Phi_J [M]^{I,T} \left\{H^{\Sigma 2}\right\} dC_I \quad \text{(V.40)}$$

This eliminates the integration over the area of the LFMVC as well as the calculation of the derivatives of the Laplace function.

Similarly, an integration by parts in (V.32) gives:

$$A_I \left\{\gamma^0\right\}^I = \sum_{J=1}^{N} [LA]^{IJ,T} [R]^I \{u\}^J - [D]^I [IH]^{I,T} \{K_\Sigma\}^I \qquad I = 1, N_C \quad \text{(V.41)}$$

with

$$[IH]^I = \begin{Bmatrix} \int_{A_I} \left\{H^{\Sigma 1}\right\}^T dA_I \\ \int_{A_I} \left\{H^{\Sigma 2}\right\}^T dA_I \end{Bmatrix} = \begin{Bmatrix} \int_{A_I} \left\langle H^{\Sigma 1}\right\rangle dA_I \\ \int_{A_I} \left\langle H^{\Sigma 2}\right\rangle dA_I \end{Bmatrix} \quad \text{(V.42)}$$

and

$$[LA]^{IJ} = \begin{bmatrix} \oint_{C_I} M_1^I \Phi^J dC_I & 0 & \oint_{C_I} M_2^I \Phi^J dC_I \\ 0 & \oint_{C_I} M_2^I \Phi^J dC_I & \oint_{C_I} M_1^I \Phi^J dC_I \end{bmatrix} \quad I = 1, N_C,\ J = 1, N \tag{V.43}$$

Using the definition of $[A]^{IJ}$ in table V.2 and introducing the angle α_I between the global and the local frames (figure V.1), we get:

$$[LA]^{IJ} = \begin{bmatrix} cos\alpha_I\, A_1^{IJ} + sin\alpha_I\, A_2^{IJ} & 0 & -sin\alpha_I\, A_1^{IJ} + cos\alpha_I\, A_2^{IJ} \\ 0 & -sin\alpha_I\, A_1^{IJ} + cos\alpha_I\, A_2^{IJ} & cos\alpha_I\, A_1^{IJ} + sin\alpha_I\, A_2^{IJ} \end{bmatrix} \tag{V.44}$$

Hence, the only terms requiring integration over a cell are $[V]^I$ and $[IH]$.

However, these terms can be integrated analytically as explained in annex 3.

Consequently, in the present theory, none of the terms requires numerical integration over the area of a cell. The only numerical integrations required are integrations over edges of the Voronoi cells.

This shows that the benefits obtained by this approach in the linear elastic domain and in the case of materially non linear problems remain valid for applications in Linear Elastic Fracture Mechanics.

V.5. Solution of the equation system

Since we consider a linear elastic material, the constitutive equation for a Voronoi cell J is:

$$\{\sigma\}^J = [C]^J \{\varepsilon\}^J \tag{V.45}$$

where $[C]^J$ is the Hooke compliance matrix of the elastic material composing cell J.

Introducing this in (V.31), we get:

$$\sum_{I=1}^{N_C} \left\{ [R]^{I,T} [W]^{IJ} \{K_\Sigma\}^I + \int_{A_I} [R]^{I,T} [\partial\Phi]^{J,T} \{P^0\}^I dA_I \right\} + \sum_{I=N_C+1}^{N} [A]^{IJ} [C^*]^I A_I \{\varepsilon\}^I - \{\tilde{F}\}^J - \{\tilde{T}\}^J - \sum_{K=1}^{M_u} B^{KJ} \{r\}^K = 0, \quad J \subset \{1, N\} \tag{V.46}$$

with

$$[C^*]^I = \frac{1}{A_I}[C]^I \tag{V.47}$$

The term $\int_{A_I} [R]^{I,T} [\partial\Phi]^{J,T} \{P^0\}^I dA_I$ of (V.46) is integrated by parts and then, the term $A_I \{\varepsilon\}^I$ given by (V.30) is introduced in (V.46). This gives:

$$\sum_{I=1}^{N_C}\left\{[R]^{I,T}\,[W]^{IJ}\{K_\Sigma\}^I+[R]^{I,T}[LA]^{IJ}\left\{P^0\right\}^I\right\}+\sum_{L=1}^{N}\left(\sum_{I=N_C+1}^{N}[A]^{IJ}\left[C^*\right]^I[A]^{IL,T}\right)\{u\}^L$$

$$-\left\{\tilde{F}\right\}^J-\left\{\tilde{T}\right\}^J-\sum_{K=1}^{M_u}B^{KJ}\{r\}^K=0,\quad J=1,N\,,\quad J\subset\{1,N\} \tag{V.48}$$

If we use the notation

$$[M]^{JL}=\sum_{I=N_C+1}^{N}[A]^{IJ}\left[\mathrm{C}^*\right]^I[A]^{IL,T} \tag{V.49}$$

this result takes the form:

$$\sum_{I=1}^{N_C}\left\{[R]^{I,T}\,[W]^{IJ}\{K_\Sigma\}^I+[R]^{I,T}[LA]^{IJ}\left\{P^0\right\}^I\right\}+$$

$$\sum_{L=1}^{N}[M]^{JL}\,\{u\}^L-\sum_{K=1}^{M_u}B^{KJ}\{r\}^K=\left\{\tilde{F}\right\}^J+\left\{\tilde{T}\right\}^J,\quad J=1,N \tag{V.50}$$

On the other hand, we have

$$e_1^I=\int_{A_I}\left\langle P^0\right\rangle[D]^I\left\{H^{\Sigma1}\right\}dA_I+K_{\Sigma1}^I\int_{A_I}\left\langle H^{\Sigma1}\right\rangle[D]^I\left\{H^{\Sigma1}\right\}dA_I+K_{\Sigma2}^I\int_{A_I}\left\langle H^{\Sigma1}\right\rangle[D]^I\left\{H^{\Sigma2}\right\}dA_I$$

$$e_2^I=\int_{A_I}\left\langle P^0\right\rangle[D]^I\left\{H^{\Sigma2}\right\}dA_I+K_{\Sigma1}^I\int_{A_I}\left\langle H^{\Sigma2}\right\rangle[D]^I\left\{H^{\Sigma1}\right\}dA_I+K_{\Sigma2}^I\int_{A_I}\left\langle H^{\Sigma2}\right\rangle[D]^I\left\{H^{\Sigma2}\right\}dA_I$$

$$\{e\}^I=\begin{Bmatrix}e_1^I\\ e_2^I\end{Bmatrix}=\left\{e^0\right\}^I+[V]^{\mathrm{I}}\{K_\Sigma\}^I \tag{V.51}$$

With this, the compatibility equation in the LFMVC (V.27) becomes:

$$\left\{e^0\right\}^I+[V]^{\mathrm{I}}\{K_\Sigma\}^I=\left\{e^0\right\}^I+\left\{e^\gamma\right\}^I+2\,[V]^I\{K_\Sigma\}-\sum_{J=1}^{N}[W]^{IJ,T}[R]^I\{u\}^{\mathrm{J}}\,,\quad I=1,N_C \tag{V.52}$$

This equation provides the stress intensity factors $\{K_\Sigma\}^I$ for crack tip *I*:

$$\{K_\Sigma\}^I=[V]^{I,-1}\left\{\sum_{J=1}^{N}[W]^{IJ,T}[R]^I\{u\}^J\right\}-[V]^{I,-1}\left\{e^\gamma\right\}^I,\quad I=1,N_C \tag{V.53}$$

Introducing, from table V.2,

$$\left\{e^\gamma\right\}^I=[IH]^I\left\{\gamma^0\right\} \tag{V.54}$$

in the above equation and combining with (V.39, V.40), we can get after some manipulations:

$$\{K_\Sigma\}^I=[VD]^{I,-1}\sum_{J=1}^{N}[WR]^J\{u\}^J \tag{V.55}$$

$$\left\{\gamma^0\right\}^I=\sum_{J=1}^{N}\left[B^0\right]^{IJ}\{u\} \tag{V.56}$$

with

$$[VD]^I = [V]^I - \frac{1}{A_I}[IH]^I[D]^I[IH]^{I,T} \tag{V.57}$$

$$[WR]^J = [W]^{IJ,T}[R]^I - \frac{1}{A_I}[IH]^I[LA]^{IJ,T}[R]^I \tag{V.58}$$

$$\left[B^0\right]^{IJ} = \frac{1}{A_I}[LA]^{IJ,T}[R]^I - \frac{1}{A_I}[D]^I[IH]^{I,T}[VD]^{I,-1}[WR]^J \tag{V.59}$$

Introducing this in (V.50) yields, after some calculations:

$$\sum_{L=1}^{N}\left\{\sum_{I=1}^{N_C}\left\{[RW]^{JL} - \frac{1}{A_I}[WA]^{JL} + \frac{1}{A_I}[RA]^{JL} - \frac{1}{A_I}[WB]^{JL} + \frac{1}{A_I^2}[RH]^{JL}\right\}\{u\}^L\right\}$$

$$+\sum_{L=1}^{N}[M]^{\mathrm{JL}}\{u\}^L - \sum_{K=1}^{M_u}B^{KJ}\{r\}^K = \left\{\tilde{F}\right\}^J + \left\{\tilde{T}\right\}^J, \quad J=1,N \tag{V.60}$$

with

$$[RW]^{JL} = [R]^{I,T}[W]^{IJ}[VD]^{I,-1}[W]^{IL,T}[R]^I \tag{V.61}$$

$$[WA]^{JL} = [R]^{I,T}[W]^{IJ}[VD]^{I,-1}[IH]^I[LA]^{IL,T}[R]^I \tag{V.62}$$

$$[WB]^{JL} = [R]^{I,T}[LA]^{IJ}[IH]^{I,T}[VD]^{I,-1}[W]^{IL,T}[R]^I \tag{V.63}$$

$$[RA]^{JL} = [R]^{I,T}[LA]^{IJ}[D]^{I,-1}[LA]^{IL,T}[R]^I \tag{V.64}$$

$$[RH]^{JL} = [R]^{I,T}[LA]^{IJ}[IH]^{I,T}[VD]^{I,-1}[IH]^I[LA]^{IL,T}[R]^I \tag{V.65}$$

If we use the notation

$$[MA]^{JL} = \sum_{I=1}^{N_C}\left\{[RW]^{JL} - \frac{1}{A_I}[WA]^{JL} + \frac{1}{A_I}[RA]^{JL} - \frac{1}{A_I}[WB]^{JL} + \frac{1}{A_I^2}[RH]^{JL}\right\} \tag{V.66}$$

then (V.60) becomes:

$$\sum_{L=1}^{N}\left\{[MA]^{JL} + [M]^{JL}\right\}\{u\}^L - \sum_{K=1}^{M_u}B^{KJ}\{r\}^K = \left\{\tilde{F}\right\}^J + \left\{\tilde{T}\right\}^J, \quad J=1,N \tag{V.67}$$

or

$$\sum_{L=1}^{N}[M_W]^{JL}\{u\}^L - \sum_{K=1}^{M_u}B^{KJ}\{r\}^K = \left\{\tilde{Q}\right\}^J, \quad J=1,N \tag{V.68}$$

with

$$[M_W]^{JL} = [MA]^{JL} + [M]^{JL}, \quad J=1,N, \quad L=1,N \tag{V.69}$$

Equations (V.33) and (V.69) constitute an equation system of the form:

$$\begin{bmatrix} [M_W] & -[B] \\ -[B]^T & [0] \end{bmatrix} \begin{Bmatrix} \{q\} \\ \{r\} \end{Bmatrix} = \begin{Bmatrix} \{\tilde{Q}\} \\ -\{\tilde{U}\} \end{Bmatrix} \tag{V.70}$$

which is similar to the one obtained in linear elasticity (III.60).

The matrix $[M_W]$ is symmetric.

Equations (V.33) which, in matrix form, become $[B]^T \{q\} = \{\tilde{U}\}$ constitute a set of constraints on the nodal displacements $\{q\}$. They can be used to remove some imposed displacements from the unknowns $\{q\}$as detailed in chapter III.

This leads to an equation system of the classical form $[M]\{q\} = \{\tilde{Q}\}$.

After solving this system, the displacements are known and (V.55) is used to compute the stress intensity coefficients $\{K_\Sigma\}^I$ at each crack tip.

V.6. Applications

V.6.1. Patch tests

In Linear Elastic Fracture Mechanics, it is possible to perform a patch test by loading a rectangular plate as shown on figure V.3. The crack thickness is assumed to be infinitely small.

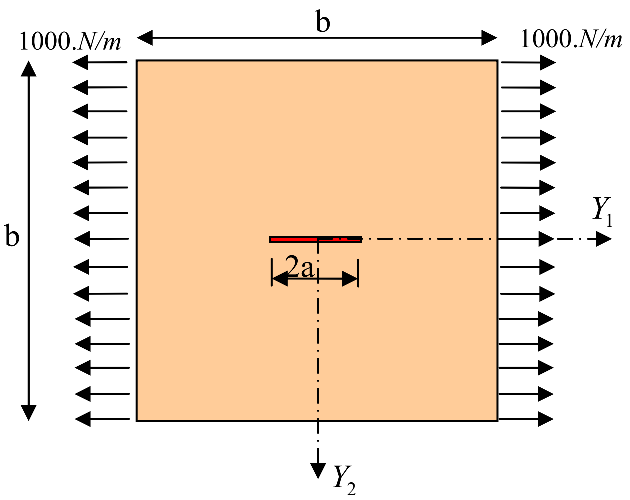

Figure V.3. Patch test loading in Linear Elastic Fracture Mechanics.

Before performing numerical patch tests, it is interesting to note that, for the loading of figure V.3, the displacement field is of the form:

$$v_1 = a_1 Y_1$$
$$v_2 = a_2 Y_2 \tag{V.71}$$

if it is expressed in the local reference system at the crack tip (Y_1, Y_2).

In such a case, we must find $K_{\Sigma 1} = K_{\Sigma 2} = 0$

More generally, if we consider a displacement field like

$$\begin{aligned} v_1 &= \alpha_1 + \beta Y_2 + a_1\, Y_1 \\ v_2 &= \alpha_2 - \beta X_1 + a_2\, Y_2 \end{aligned} \tag{V.72}$$

combining the patch test loading with the 3 rigid body modes (translations α_1 and α_2 plus rotation β), we also expect that $K_{\Sigma 1} = K_{\Sigma 2} = 0$.

Below, it is proved analytically that it is the case with the present numerical approach.

The compatibility equations (V.27) for the LFMVCs can be written:

$$\{e\}^I = \left\{e^0\right\}^I + \left\{e^\gamma\right\}^I + 2\,[V]^I\,\{K_\Sigma\} - \sum_{J=1}^{N} [W]^{IJ,T}\,\{v\}^J\ ,\quad I = 1, N_C \tag{V.73}$$

with

$$\{v\}^J = [R]^I\,\{u\}^J \tag{V.74}$$

Introducing (V.18) in the definition of $\{e\}^I$ given in table V.2, we get:

$$\{e\}^I = [IH]^I\,[D]^I\left\{P^0\right\}^I + [V]^{I,T}\begin{Bmatrix} K_{\Sigma 1} \\ K_{\Sigma 2} \end{Bmatrix} \tag{V.75}$$

With this result, we get:

$$\{e\}^I - \left\{e^0\right\}^I - \left\{e^\gamma\right\}^I = [V]^{I,T}\{K_\Sigma\} - [IH]^I\left\{\gamma^0\right\} \tag{V.76}$$

Combining (V.73) and (V.76), we get:

$$[V]^{I,T}\{K_\Sigma\} - [IH]^I\left\{\gamma^0\right\} = 2\,[V]^I\,\{K_\Sigma\} - \sum_{J=1}^{N} [W]^{IJ,T}\,\{v\}^J\ ,\quad I = 1, N_C$$

Taking account of the symmetry of $[V]^I$, the following equation is obtained:

$$[V]^I\,\{K_\Sigma\} = \sum_{J=1}^{N} [W]^{IJ,T}\,\{v\}^J - [IH]^I\left\{\gamma^0\right\}\quad I = 1, N_C \tag{V.77}$$

With the definition of $[W]$ in table V.2 and (V.39, V.40), we get:

$$[W]^{IJ,T} = \begin{bmatrix} \oint_{C_I} \Phi_J\,(M_1^I H_{11}^{\Sigma 1} + M_2^I H_{12}^{\Sigma 1})\,dC_I & \oint_{C_I} \Phi_J\,(M_2^I H_{22}^{\Sigma 1} + M_1^I H_{12}^{\Sigma 1})\,dC_I \\ \oint_{C_I} \Phi_J\,(M_1^I H_{11}^{\Sigma 2} + M_2^I H_{12}^{\Sigma 2})\,dC_I & \oint_{C_I} \Phi_J\,(M_2^I H_{22}^{\Sigma 2} + M_1^I H_{12}^{\Sigma 2})\,dC_I \end{bmatrix} \tag{V.78}$$

Now, we can calculate:

$$\sum_{J=1}^{N} [W]^{IJ,T}\,\{v\}^J$$

$$= \begin{Bmatrix} \oint_{C_I} \sum_{J=1}^{N} \Phi_J v_1^J \ (M_1^I H_{11}^{\Sigma 1} + M_2^I H_{12}^{\Sigma 1})dC_I + \oint_{C_I} \sum_{J=1}^{N} \Phi_J v_2^J \ (M_2^I H_{22}^{\Sigma 1} + M_1^I H_{12}^{\Sigma 1})dC_I \\ \oint_{C_I} \sum_{J=1}^{N} \Phi_J v_1^J \ (M_1^I H_{11}^{\Sigma 2} + M_2^I H_{12}^{\Sigma 2})dC_I + \oint_{C_I} \sum_{J=1}^{N} \Phi_J v_2^J \ (M_2^I H_{22}^{\Sigma 2} + M_1^I H_{12}^{\Sigma 2})dC_I \end{Bmatrix}$$

$$= \begin{Bmatrix} \oint_{C_I} v_1 (M_1^I H_{11}^{\Sigma 1} + M_2^I H_{12}^{\Sigma 1})dC_I + \oint_{C_I} v_2 (M_2^I H_{22}^{\Sigma 1} + M_1^I H_{12}^{\Sigma 1})dC_I \\ \oint_{C_I} v_1 (M_1^I H_{11}^{\Sigma 2} + M_2^I H_{12}^{\Sigma 2})dC_I + \oint_{C_I} v_2 (M_2^I H_{22}^{\Sigma 2} + M_1^I H_{12}^{\Sigma 2})dC_I \end{Bmatrix} \quad \text{(V.79)}$$

Integrating by parts yields:

$$\sum_{J=1}^{N} [W]^{IJ,T} \{v\}^J = \begin{Bmatrix} \int_{A_I} \left(H_{11}^{\Sigma 1} \frac{\partial v_1}{\partial Y_1} + H_{12}^{\Sigma 1} (\frac{\partial v_1}{\partial Y_2} + \frac{\partial v_2}{\partial Y_1}) + H_{22}^{\Sigma 1} \frac{\partial v_2}{\partial Y_2} \right) dA_I \\ \int_{A_I} \left(H_{11}^{\Sigma 2} \frac{\partial v_1}{\partial Y_1} + H_{12}^{\Sigma 2} (\frac{\partial v_1}{\partial Y_2} + \frac{\partial v_2}{\partial Y_1}) + H_{22}^{\Sigma 2} \frac{\partial v_2}{\partial Y_2} \right) dA_I \end{Bmatrix} \quad \text{(V.80)}$$

For the particular case of the displacements (V.74), (V.80) becomes

$$\sum_{J=1}^{N} [W]^{IJ,T} \{v\}^J = \begin{Bmatrix} \int_{A_I} \left(a_1 H_{11}^{\Sigma 1} + a_2 H_{22}^{\Sigma 1} \right) dA_I \\ \int_{A_I} \left(a_1 H_{11}^{\Sigma 2} + a_2 H_{22}^{\Sigma 2} \right) dA_I \end{Bmatrix} \quad \text{(V.81)}$$

On the other hand, equation (V.32) gives:

$$A_I \left\{ \gamma^0 \right\}^I = \sum_{J=1}^{N} \int_{A_I} [\partial \Phi]^J dA_I \ \{v\}^J - [D]^I [IH]^{I,T} \{K_\Sigma\}^I \quad I = 1, N_C \quad \text{(V.82)}$$

or :

$$\left\{ \gamma^0 \right\}^I = \frac{1}{A_I} \begin{Bmatrix} \int_{A_I} \frac{\partial v_1}{\partial Y_1} dA_I \\ \int_{A_I} \frac{\partial v_2}{\partial Y_2} dA_I \\ \int_{A_I} \frac{\partial v1}{\partial Y_2} dA_I + \int_{A_I} \frac{\partial v_2}{\partial Y_1} dA_I \end{Bmatrix} - \frac{1}{A_I} [D]^I [IH]^{I,T} \{K_\Sigma\}^I \quad I = 1, N_C \quad \text{(V.83)}$$

If we pre-multiply by $[IH]^I$, (V.83) becomes :

$$[IH]^I\left\{\gamma^0\right\}^I=\frac{1}{A_I}[IH]^I\begin{Bmatrix}\int_{A_I}\frac{\partial v_1}{\partial Y_1}dA_I\\ \int_{A_I}\frac{\partial v_2}{\partial Y_2}dA_I\\ \int_{A_I}\frac{\partial v1}{\partial Y_2}dA_I+\int_{A_I}\frac{\partial v_2}{\partial Y_1}dA_I\end{Bmatrix}-\frac{1}{A_I}[IH]^I[D]^I[IH]^{I,T}\{K_\Sigma\}^I \qquad (V.84)$$

For the particular case of the displacements (V.74), (V.84) becomes

$$[IH]^I\left\{\gamma^0\right\}^I=\begin{Bmatrix}\int_{A_I}\left(a_1H_{11}^{\Sigma 1}+a_2H_{22}^{\Sigma 1}\right)dA_I\\ \int_{A_I}\left(a_1H_{11}^{\Sigma 2}+a_2H_{22}^{\Sigma 2}\right)dA_I\end{Bmatrix}-\frac{1}{A_I}[IH]^I[D]^I[IH]^{I,T}\{K_\Sigma\}^I,\ I=1,N_C \qquad (V.85)$$

Replacing (V.85) and (V.81) in (V.77) gives :

$$\left([V]^I-\frac{1}{A_I}[IH]^I[D]^I[IH]^{I,T}\right)\{K_\Sigma\}^I=0 \quad I=1,N_C \qquad (V.86)$$

It is easy to see that, in this equation, the matrix $\left([V]^I-\frac{1}{A_I}[IH]^I[D]^I[IH]^{I,T}\right)$ is regular.

This proves that $\{K_\Sigma\}=0$ if the displacement field is a rigid body mode or corresponds to a patch test loading.

It must be noted that the analytical development above implies the exact evaluation of all the terms involved in the equations used.

This is the case for $[V]^I$ and $[IH]^I$ which are calculated analytically (annex 3) but not for the other terms that imply a numerical integration on the contours or the edges of the Voronoi cells.

Consequently, in practice, $\{K_\Sigma\}$ will be only approximately equal to zero, the degree of approximation depending on the precision of the numerical integration scheme.

To evaluate this, a number of numerical patch tests (figure V.3) are performed. The Voronoi cells are shown in figure V.4 where only a quarter of the domain is studied by symmetry. The crack is represented by a thick red line but, in the computations, its thickness is equal to zero.

The results in figures V.5, V.6, V.7 show the evolution of $\{K_\Sigma\},\{P_0\},\{\sigma\}$ for different numbers of integration points (nb of IP) on the edges of the LFMVC located at the crack tip and on the edges of the OVCs. This evolution is expressed with the help of the following variables:

$$L2\_\sigma=\frac{\sum_{K=1}^{N}A_K\sqrt{(\sigma_{ij}^K-\sigma_{ij}^{exact})(\sigma_{ij}^K-\sigma_{ij}^{exact})}\Big/\sum_{K=1}^{N}A_K}{\sum_{K=1}^{N}A_K\sqrt{\sigma_{ij}^{exact}\sigma_{ij}^{exact})}\Big/\sum_{K=1}^{N}A_K} \qquad (V.87)$$

$$L2\_P^0 = \frac{\sqrt{(P^0{}_{ij} - P^0{}_{ij}^{exact})(P^0{}_{ij}^{K} - P^0{}_{ij}^{exact})}}{1000} \qquad \text{(V.88)}$$

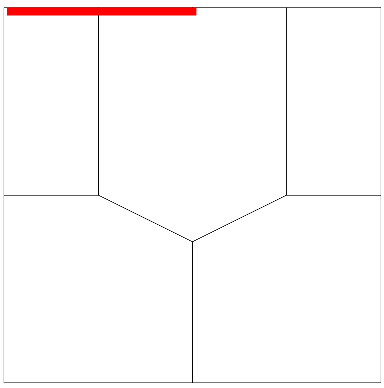

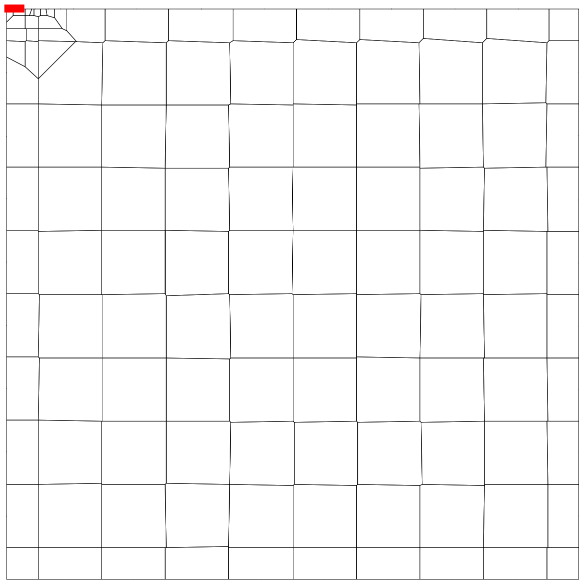

Case 1: 5 cells Crack length: a=400mm; Domain size: b=800mm;	Case 2: 116 cells Crack length: a=5mm; Domain size: b=100mm

Figure V.4. Numerical patch tests

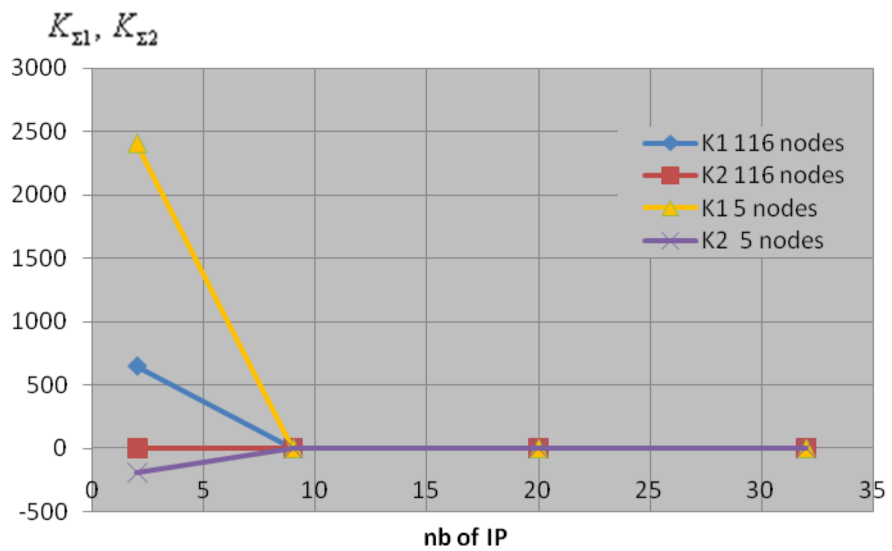

Figure V.5. Patch tests: convergence of $K_{\Sigma1}$

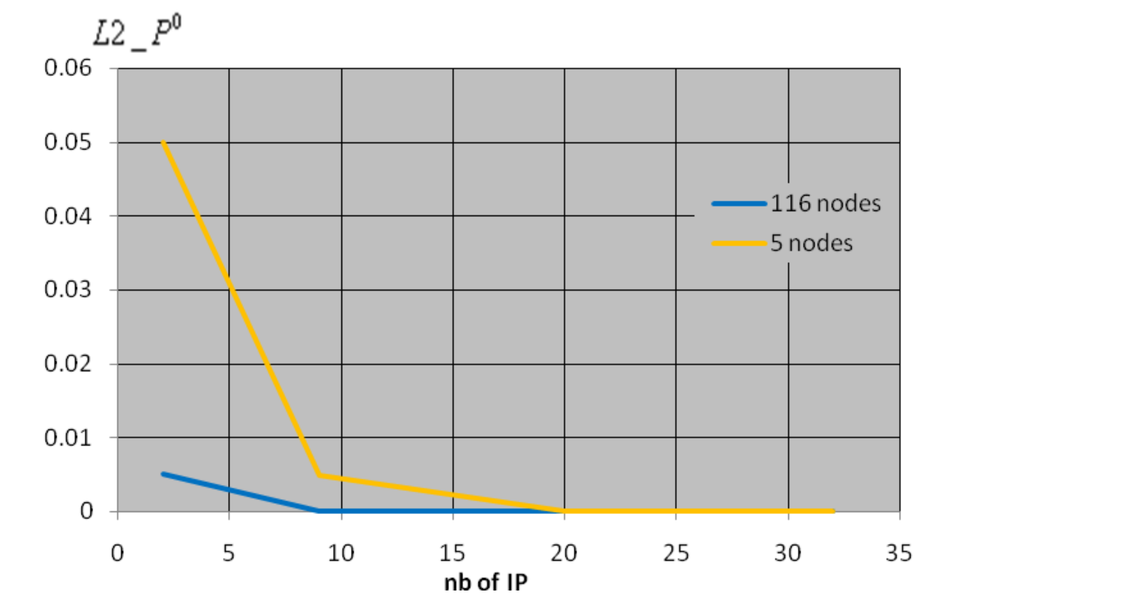

Figure V.6. Patch tests: convergence of P_0

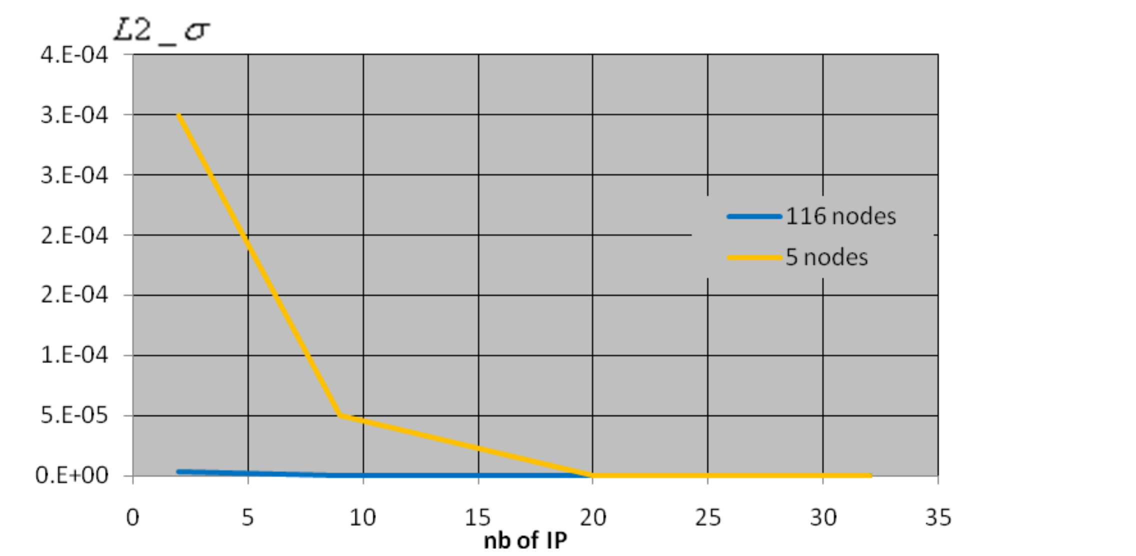

Figure V.7. Patch tests: convergence of σ

V.6.2. Translation tests

If we impose $a_1 = a_2 = \beta = 0$ in (V.72), the displacement field reduces to a translation. Introducing these conditions in (V.81), we get:

$$\sum_{J=1}^{N} [W]^{IJ,T} = 0 \qquad \text{(V.89)}$$

Again, this is valid if all the integrations are performed exactly but is only an approximation if numerical integration is used.

A series of translation tests ($u_x = 1\,mm;\ u_y = 0\,mm$ on all the nodes) with different numbers of cells are performed to evaluate the performance of the numerical integration.

Figure V.8 shows the configuration with 12 cells. Figure V.9 illustrates the models with 196 and 316 nodes.

Figures V.10 and V.11 show the evolution of $K_{\Sigma 1}$ and $\sum_{J=1}^{N} [W]^{IJ,T}$ for different numbers of nodes and different numbers of integration points respectively.

Some results are extremely close to each other so that it is hard to see the difference between the curves.

For all the cases, $K_{\Sigma 2}$ is equal to zero within machine presicion.

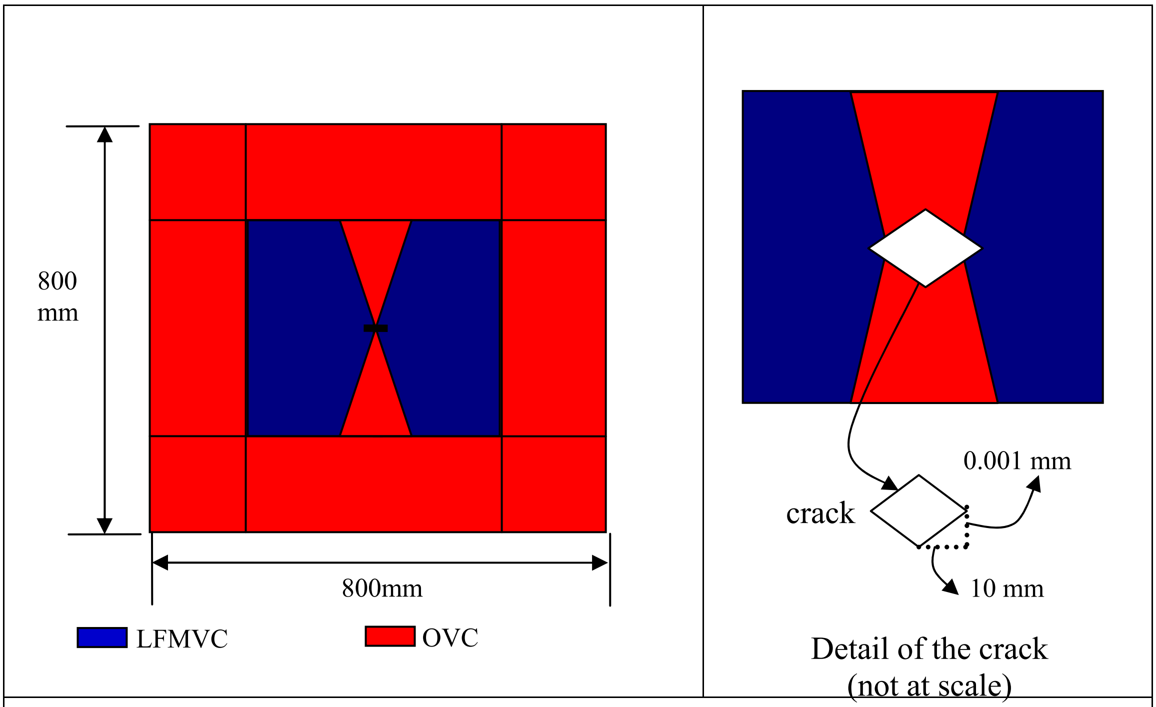

Figure V.8. Geometry and Voronoi cells for 12 nodes

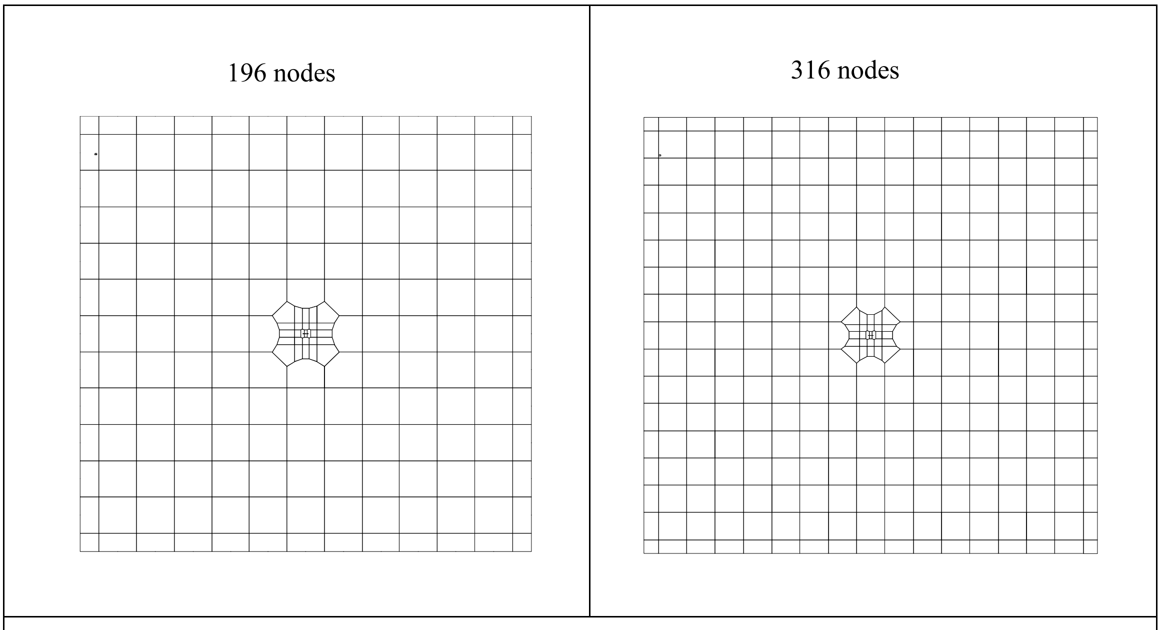

Figure V.9. Voronoi cells for 196 and 316 nodes

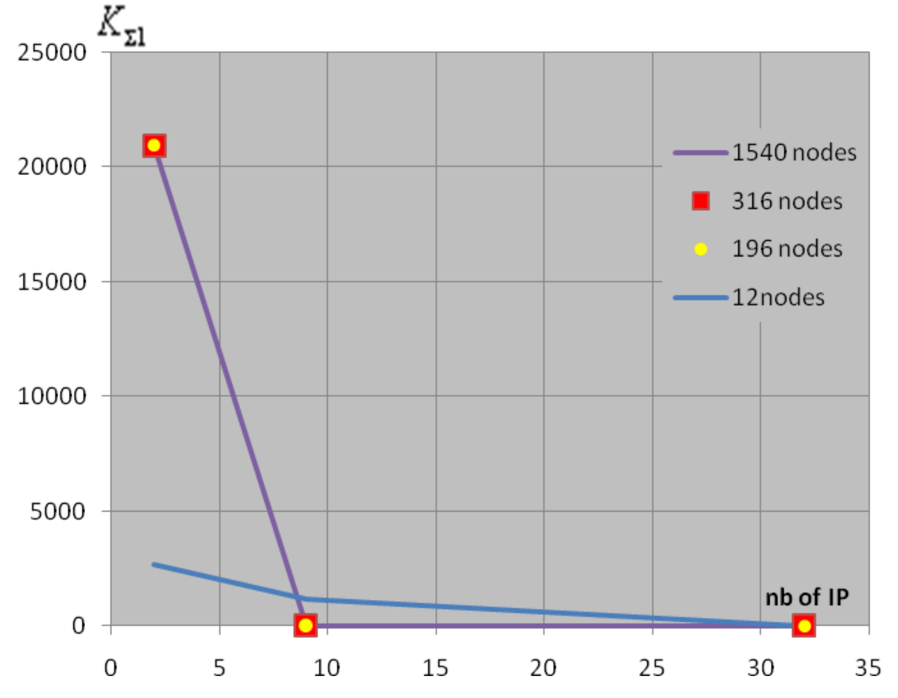

Figure V.10. Convergence on $K_{\Sigma 1}$ for translation

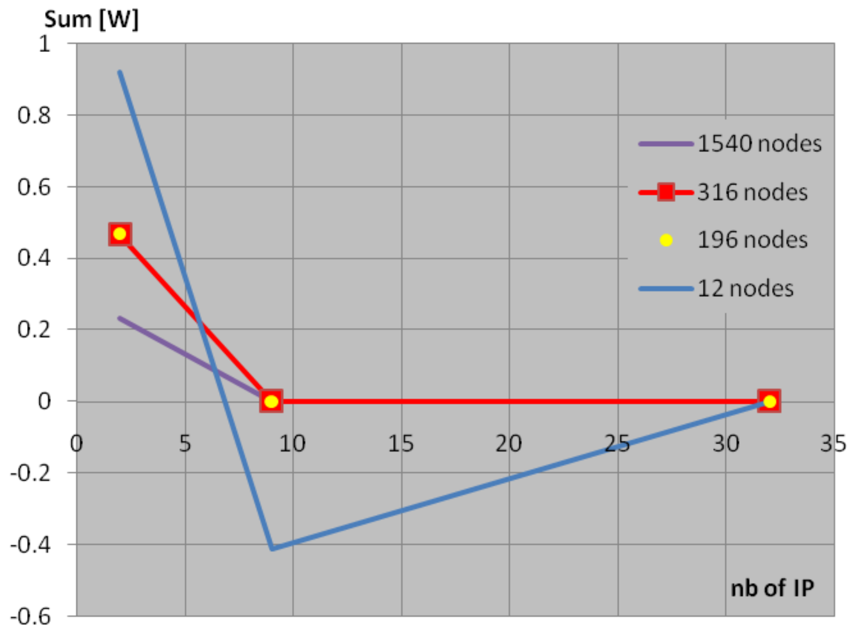

Figure V.11. Convergence on $Sum[W] = \sum_{J=1}^{N} [W]^{IJ,T}$ for translation

V.6.3. Mode 1 tests

With the same models as in the translation case, we can perform numerical tests for mode 1 as shown in figure V.12.

Theoretically, $K_{\Sigma 1} = \sigma_\infty \sqrt{\pi a}$ and $K_{\Sigma 2} = 0$ with $\sigma_\infty = 1000\ N/mm^2$ and $a = 10\ mm$.

For the numerical calculations, plane stress state was assumed and the values of Young's modulus and Poisson's ratio were:

$E = 200000\ MPa$ and $\nu = 0.3$

but these assumption have no influence on the values of the stress intensity coefficients.

Figure V.13 shows the convergence on $K_{\Sigma 1}$ with different numbers of nodes and 2 Gauss integration points on the edges of the Voronoi cells. Figure V.14 shows the convergence on $K_{\Sigma 1}$ for 12 nodes using the trapeze integration scheme on the edges of the LFMVC and 2 Gauss points on the edges of the OVCs

The superiority of the Gauss scheme over the trapeze scheme is obvious from figure V.14.

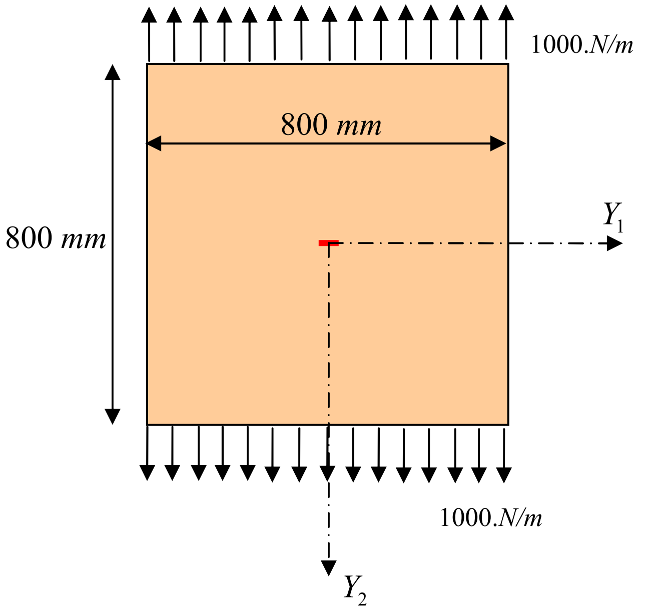

Figure V.12.Mode 1 test loading in linear fracture mechanics. The details of crack geometry are given in figure V.8.

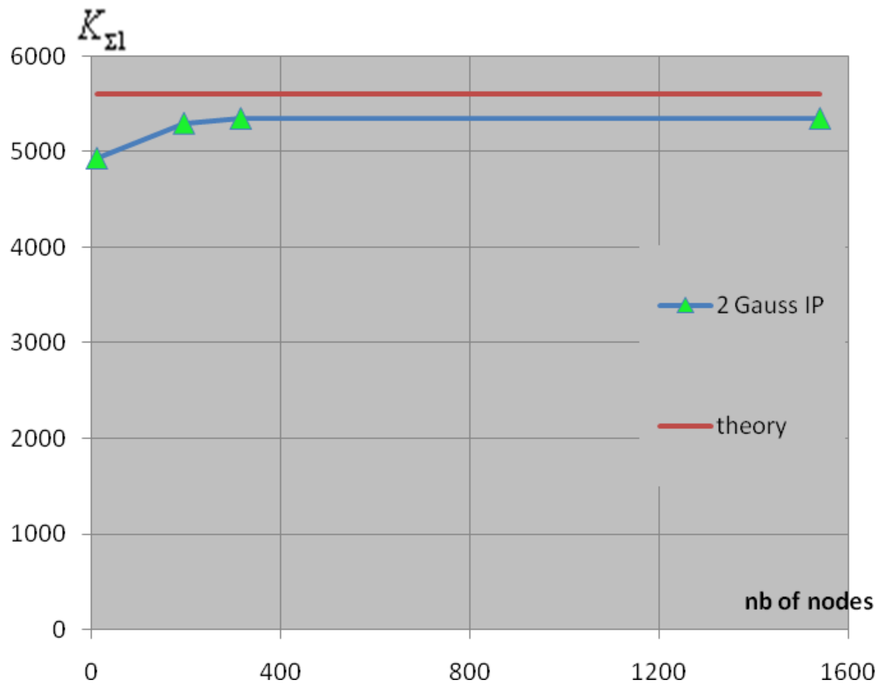

Figure V.13. Convergence on $K_{\Sigma 1}$ for mode 1

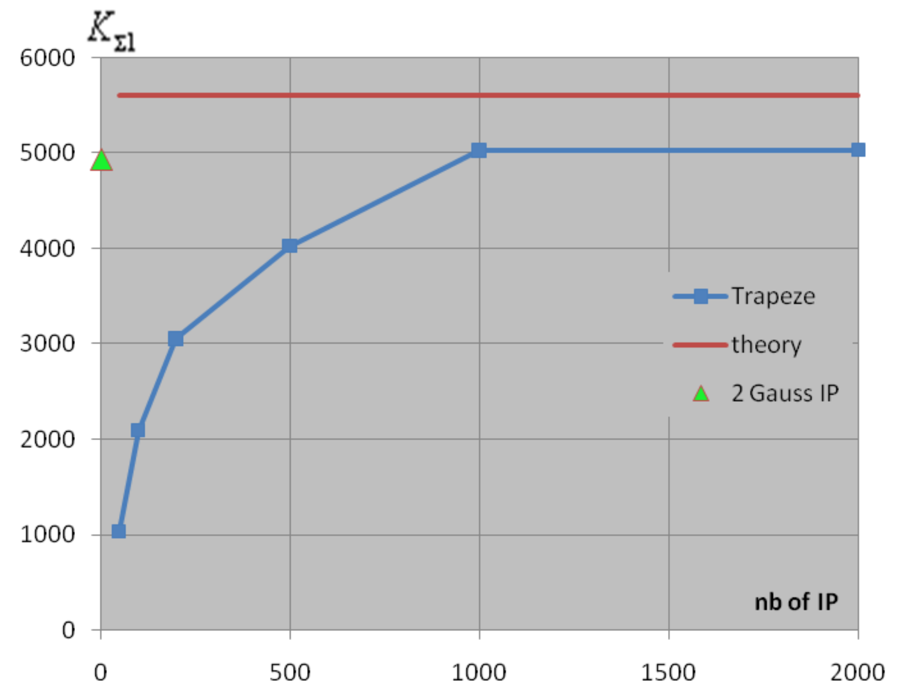

Figure V.14. Convergence on $K_{\Sigma 1}$ for mode 1 (12 nodes)

V.6.4. Mode 2 tests

With the same models as in the translation case, we can perform numerical tests for mode 2 as shown in figure V.15.

The values of Young's modulus and Poisson's ratio are the same as for mode 1 patch test.

Plane stress state was also assumed.

Theoretically, $K_{\Sigma 2} = \tau_{\infty}\sqrt{\pi a}$ and $K_{\Sigma 1} = 0$ with $\tau_{\infty} = 1000\ N/mm^2$ and $a = 10\,mm$.

Figure V.16 shows the convergence on $K_{\Sigma 2}$ with different numbers of nodes and different numbers of Gauss integration points on the edges of the Voronoi cells.

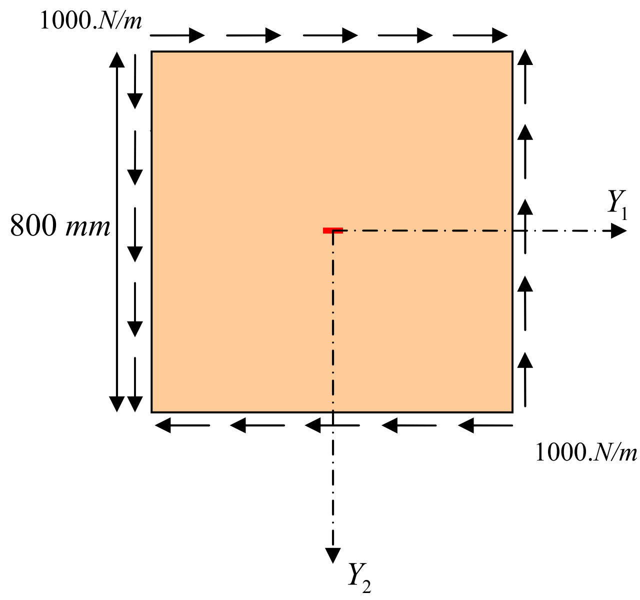

Figure V.15. Mode 2 test loading in Linear Elastic Fracture Mechanics. The details of crack geometry are given in figure 8

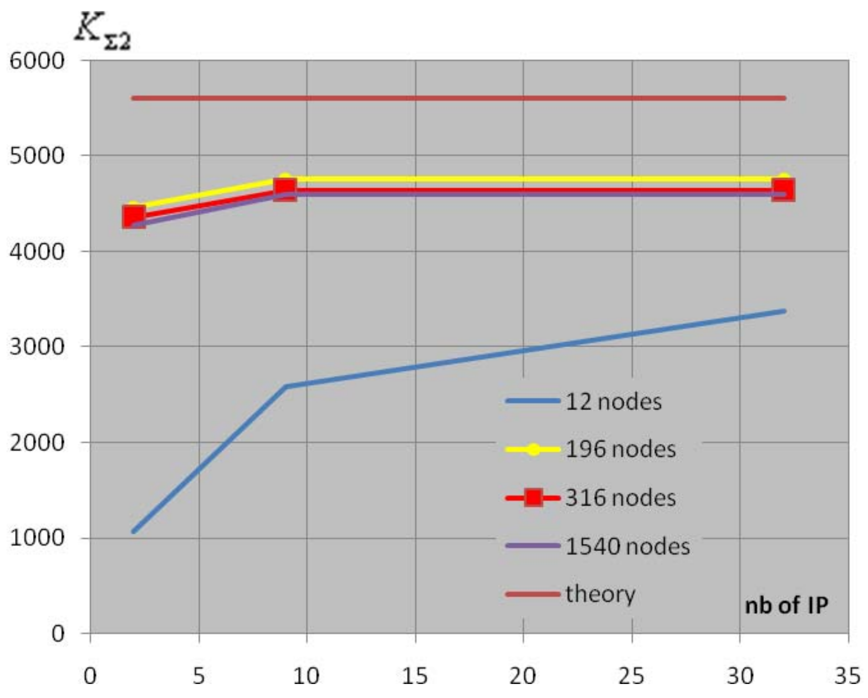

Figure V.16. Convergence on $K_{\Sigma 2}$ for mode 2

V.6.5. Bar with a single edge crack

The problem of figure V.17 is treated as a last example.

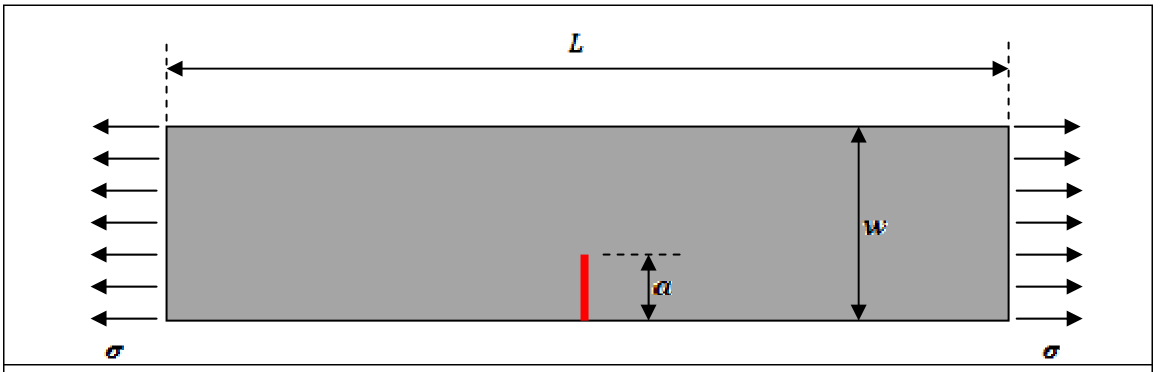

Figure 17. Bar with a single edge crack (not at scale)

The crack (in red) has no thickness and is located at mid span.

The values used for the computations are:

$L = 1600\ mm; w = 400mm; a = 10\ mm, \sigma = 1000\ MPa$

$E = 200000\ MPa$ and $\nu = 0.3$

Plane stress state is considered.

The theoretical value of the stress intensity coefficient is given in [MIANNAY D. P. (1998)] for $L \to \infty$:

$$K_I = \sigma\sqrt{w}\,\frac{\sqrt{2tg\frac{\pi a}{w}}}{cos\frac{\pi a}{w}}\left[0.752 * 2.02 * \frac{a}{w} + 0.37 * (1 + sin\frac{\pi a}{w})^3\right] \qquad (V.90)$$

The computations were performed for different numbers of nodes and different numbers of integration points on the edges of the LFMVC.

Figure V.18 shows the Voronoi cells for 17 nodes and 316 nodes.

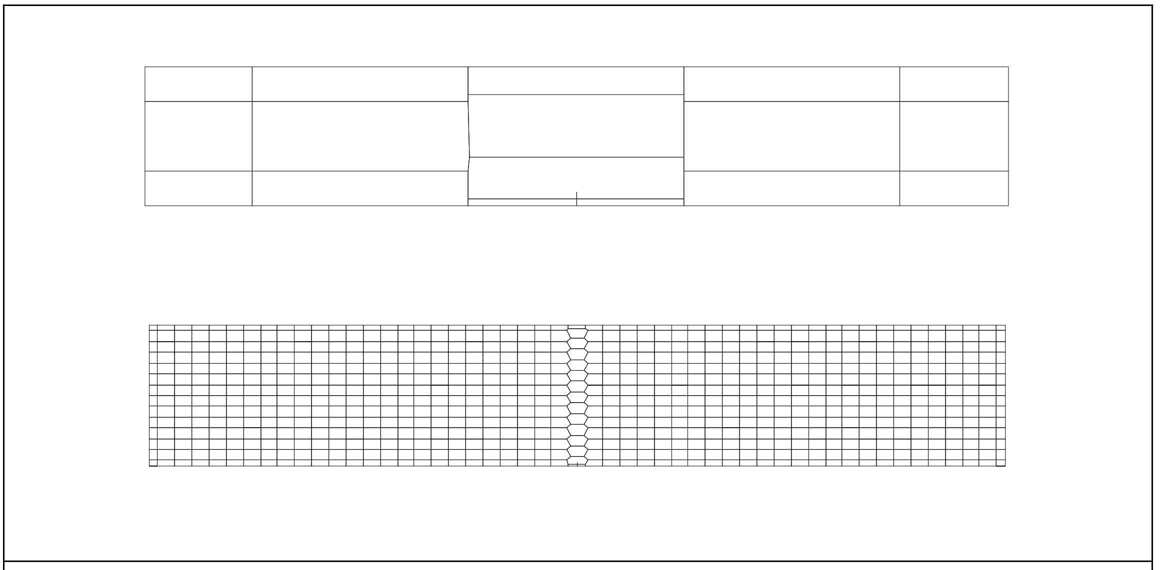

Figure V.18. Voronoi cells for 17 nodes and 316 nodes

The values of the stress intensity coefficient obtained are collected in table V.3.

Table V.3. Stress intensity coefficient for the single edge crack problem

Nb of IP	17 nodes	116 nodes	352 nodes	718 nodes	Theory
2	156	743	1038	1503	6344
9	2201	5124	5288	5560	6344
32	3630	5569	5886	6056	6344

The convergence on the stress intensity coefficient is summarized in the diagram of figure V.19.

It is seen that the number of Gauss integration points on the edges of the LFMVC plays a significant role on the accuracy of the stress intensity coefficient.

Since the number of edges of the LFMVC is rather small, using a large number of integration points is not a real problem for the computation time.

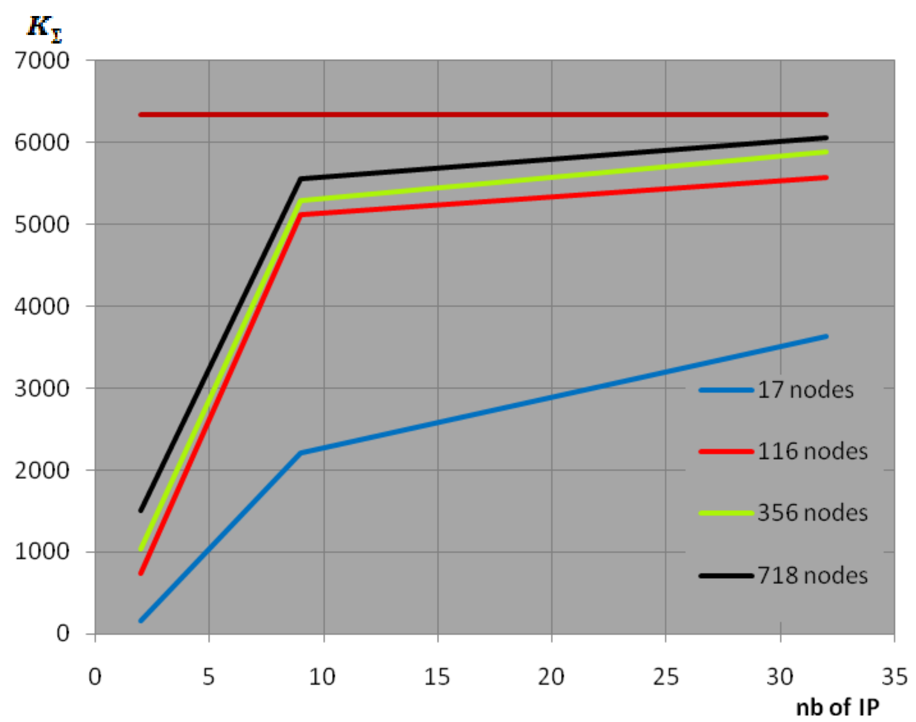

Figure V.19. Convergence of the stress intensity factor

V.6.6. Nearly incompressible material

It has been shown in chapter III that incompressibility locking is avoided in the OVCs;

In order to check that incompressibility locking is also avoided in the present case, the mode 1 test (figure V.12) has been performed for a Poisson's ratio close to 0.5.

The results for 196 nodes are summarized in figure V.20.

It is seen that there is no incompressibility locking.

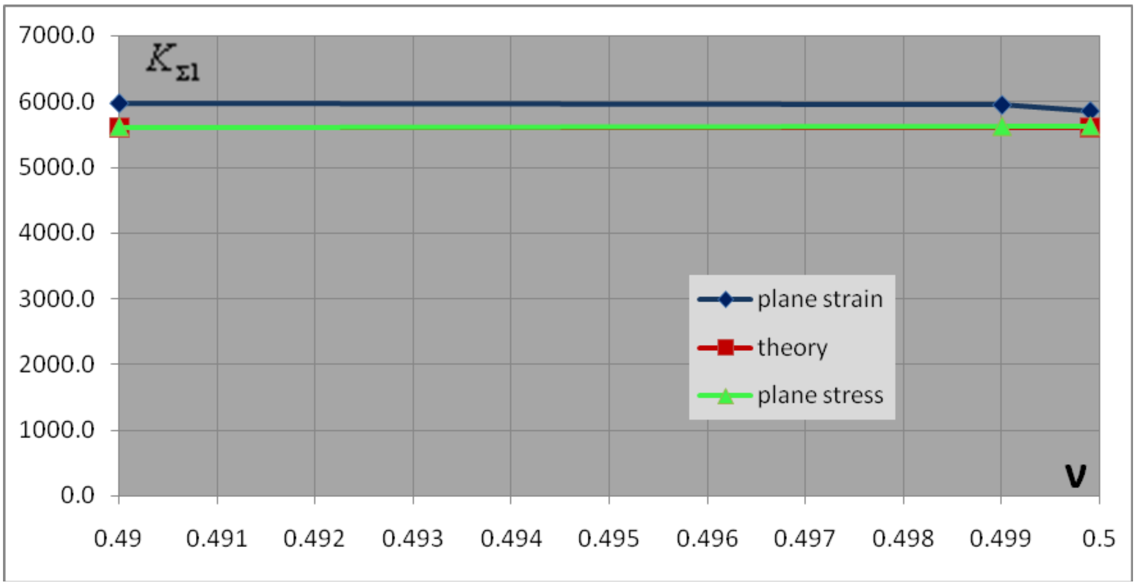

Figure 20. Mode 1 test for a nearly incompressible material

V.7. Remark

All the tests above have been performed using the discretization proposed in section V.4.

In particular, the interpolation of the displacements is given by (V.17)

$$v_i = \sum_{J=1}^{N} \Phi_J v_i^J$$

An attempt has been made to enrich the discretization of the displacements near the crack tip nodes by terms of the form:

$$\begin{Bmatrix} u_1 \\ u_2 \end{Bmatrix}_K = \left[\frac{K_{\Sigma 1}}{2\mu}\sqrt{\frac{r}{2\pi}} \begin{Bmatrix} \left[\kappa - 1 + 2(sin\frac{\theta}{2})^2\right] cos\frac{\theta}{2} \\ \left[\kappa + 1 - 2(cos\frac{\theta}{2})^2\right] sin\frac{\theta}{2} \end{Bmatrix} + \frac{K_{\Sigma 2}}{2\mu}\sqrt{\frac{r}{2\pi}} \begin{Bmatrix} \left[\kappa + 1 + 2(cos\frac{\theta}{2})^2\right] sin\frac{\theta}{2} \\ \left[-\kappa + 1 + 2(sin\frac{\theta}{2})^2\right] cos\frac{\theta}{2} \end{Bmatrix} \right] \Phi_K$$

corresponding to the solution of LEFM in the vicinity of the crack tip.

Unfortunately, this enrichment does not provide significant improvement of the results while the development of the equations of this method becomes much more complex.

In some tests cases where the LFMVC is large (as, for example, in figure V.8), the quality of the results was even lower, probably because the above enrichment is only valid for small values of the polar coordinate *r*.

Consequently, this approach was abandoned.

V.8. Conclusion

The Fraeijs de Veubeke variational principle has been used to develop a constraint natural neighbours method in which the displacements, stresses, strains and surface support reactions can be discretized separately.

The additional degrees of freedom linked with the assumed stresses and strains can be eliminated at the level of the Voronoi cells, finally leading to a system of equations of the same size as in the classical displacement-based method.

In the application to linear fracture mechanics, in the Voronoi cells at the crack tip, an assumption on the stresses deduced from the exact solution of Westergaard [WESTERGAARD, H.M. (1939)] has been introduced by which the stress intensity coefficients become primary variables of the method. In this case, some integrals over the area of this crack tip cell remain but they can be calculated analytically so that, in the formulation, only numerical integrations on the edges of the Voronoi cells are required.

In all the cases, the derivatives of the nodal shape functions are not required in the resulting formulation.

As same as in the problems of linear elasticity and elasto-plasticity, the displacements can be imposed in 2 ways in the linear fracture problems.

- In the spirit of the FdV variational principle, boundary conditions of the type $u_i = \tilde{u}_i$ on S_u can be imposed in the average sense; hence, any function $\tilde{u}_i = \tilde{u}_i(s)$ can be accommodated by the method;
- However, since the natural neighbours method is used, the interpolation of displacements on the solid boundary is linear between 2 adjacent nodes. So, if the imposed displacements $\tilde{u}_i$ are linear between 2 adjacent nodes, they can be imposed exactly. This is obviously the case with $\tilde{u}_i = 0$. In such a case, it is equivalent to impose the displacements of these 2 adjacent nodes to zero.

Patch tests, translation tests, mode 1 tests, mode 2 tests and single edge crack tests confirm the validity of this approach.